**ORIGINAL PAPER**

# Modeling and multi-objective optimization of cutting parameters using response surface method for milling of medium carbon steel (EN8)

**N. L. Bhirud**[1] · **A. S. Dube**[1] · **Amit S. Patil**[2] · **K. S. Bhole**[2]

## Abstract

Continuous growth of the manufacturing sector is resulting in to higher energy demand due to which the manufacturing costs and greenhouse gas emissions are also increasing. Beside reduction in energy consumption; improvement in energy efficiency, power factor and reduction in cutting temperatures are also vital to ensure better sustainability of the machining sector. This work evaluates the trade-offs between energy, heat generation and cutting quality during milling of medium carbon steel (EN8) alloy steel. The effects of input process parameters viz. spindle speed, feed rate, axial depth of cut, radial depth of cut and tool helix angle has been studied on the energy consumption, energy efficiency, power factor, cutting temperatures, surface roughness response parameters. The inclusion of helix angle as an input factor and, using energy efficiency and power factor as output parameters are the major highlights of this work. The machining experiments were conducted using response surface methodology for design of experiments. The multi objective optimization was carried out by using desirability approach, for three different groups of response variables considering the different importance of energy consumption, cutting temperatures and surface roughness, under different manufacturing circumstances. The predictability of the multiple regression approach was found to be more than 90% for all the responses which highlights model significance. The direct and interaction effect were studied and discussed in details for all the responses. The values of the composite desirability achieved in all the three types of optimization problems were on higher side (0.813, 1 and 0.794). The results of the optimization were confirmed by conducting the experiments the optimized settings. The percentage error between experimental and RSM predicted result was found to be within acceptable limits. This study can be helpful for reducing the energy consumption and cutting temperature without compromising on surface roughness, in the machining of medium carbon steel.

**Keywords** End milling · Energy consumption · Energy efficiency · Power factor · Cutting temperature · Predictive modelling · Multi-objective optimization

## Abbreviations

| | |
|---|---|
| ANOVA | Analysis of variance |
| CE | Cutting energy |
| CCD | Central composite design |
| CCRD | Central composite rotatable design |
| DoE | Design of experiment |
| EE | Energy efficiency |
| F | Feed rate |
| GA | Genetic algorithm |
| H | Helix angle |
| MRR | Material removal rate |
| N | Spindle speed |
| NSGA-II | Non-dominated sorting genetic algorithm-II |
| PF | Power factor |

✉ N. L. Bhirud
niteenbhirud@gmail.com

A. S. Dube
anildube100@gmail.com

Amit S. Patil
amitpatil36@hotmail.com

K. S. Bhole
kiran_bhole@spce.ac.in

[1] Department of Mechanical Engineering, Sandip Institute of Engineering and Management, Nashik, affiliated to Savitribai Phule University of Pune, Pune, Maharashtra, India

[2] Department of Mechanical Engineering, Sardar Patel College of Engineering, Andheri, Mumbai 400058, India

PCM     Power consumed for actual cutting of material (in Watt)

PCA     Power consumed by the machine during air cutting (no workpiece)

PC     Power consumed for cutting

Ra     Surface roughness

SEC     Specific energy consumption

SA     Simulated annealing

TECM     Total energy consumption during machining

T     Workpiece surface temperature rise

Y     Radial depth of cut

Z     Axial depth of cut

# 1 Introduction

As the manufacturing sector is growing, the energy demand by this sector is also growing. Higher consumption of energy results in increase in the manufacturing costs as well as the greenhouse gas emissions. Among the diverse segments of manufacturing, machining is responsible for massive energy consumption. Thus, in the recent years, reduction in the energy demand in this segment, is a major challenge for industries as well as the researchers [1]. The optimum value of cutting parameters if chosen, could reduce about 6 to 40% energy during machining [2, 3], so this selection is vital for all the major machining operations. Milling; particularly the end milling is one amongst the foremost versatile and major machining operations used in aerospace and automotive industries for creating deep slots, profile recesses, steps etc.[4]. In the last few years, the researchers have started focusing on the reduction in the energy consumption of milling processes.

Kuram et al. [5], have used the D-optimal design of experiment (DoE) for developing second order models for tool wear, specific energy, and surface roughness during end milling of AISI 304. Cutting speed, feed, depth of cut and type of cutting fluid were used as the input variables. Both mono objective and multi objective optimization were carried out for minimization of consumed energy, tool wear and surface roughness. In another work, Campatelli et al. [6] have developed response surface models for energy consumption for spindle and axis and specific energy consumption (SEC). Also, the models for total energy consumption and total SEC were developed. The input variables were the spindle speed, feed rate, radial depth of cut and axial depth of cut. It was recommended to use higher values of process parameters in order to get minimum specific energy consumption.

Yan et al. [7], have developed models for addressing the trade- off between energy, production rate and surface quality for C-45 steel using spindle speed, feed rate and radial depth of cut and axial depth of cut as input variables. The multi

objective optimization problem was solved using weighted Gray relational analysis. The results were compared with the results of traditional optimization with MRR and roughness as objective functions and it was found that there was significant reduction in the cutting energy with the proposed analysis. Zhang et al. [8], have carried out experimental investigation and multi objective optimization for minimization of surface roughness, SEC, and maximization of MRR using hybrid non –dominated Sorting Genetic algorithm-II (NSGA-II). Ozturk et al. [9] have also carried out optimization of the cutting speed, feed rate and depth of cut for simultaneous minimization of surface roughness and energy consumption for aluminium alloy-6061.

Kadirgama et al. [10, 11] have proposed first and second order models for power consumption, torque and cutting force using RSM. Cutting speed, feed, radial depth of cut and axial depth of cut were the input parameters used for milling of stainless steel. The prediction accuracy of the second order models was noticed to be better as compared to first order models. Bagcı et al. [12] have carried out experimental studies using full factorial design with cutting speed, feed, and depth of cut as input parameters and tool wear, cutting force and power as response parameters during symmetric and asymmetric milling of Stellite-6 using coated and uncoated inserts. Ahmed et al. [13] have used Taguchi's L9 orthogonal array for minimization of the surface roughness and energy consumption with the cutting speed, feed rate, and depth of cut as the process variables. In another study by Rizal et al. [14] carried out experimental work for minimization of material removal rate and power consumption during slot milling of aluminium 6061 alloy using the feed rate, axial depth of cut and radial depth of cut as the process parameters.

In the work carried by, Sahu et al. [15], Ti-6Al-4V titanium alloy was machined using cutting speed, feed, and depth of cut as input parameters and surface roughness, tool wear, power consumption and MRR as responses. The multiobjective optimization of the developed regression models was carried out using the desirability function approach. The error in the predicted and experimental results was found to be less than 8.2%. Malghan et al. [16] have carried out milling on aluminium matrix composites with feed rate, spindle speed and depth of cut as input factors and cutting force, surface roughness and power consumption as responses using RSM. The optimization was carried out using the desirability approach and particle swarm optimization (PSO). It was noticed that spindle speed has played major role on all the responses which was followed by feed rate and depth of cut.

The major focus of researchers was on the reduction of energy consumption and SEC, but the important parameters like energy efficiency (EE) and power factor are overlooked. The energy efficiency is defined as; the ratio of the effective energy consumed during actual cutting process to total

energy consumed by the machine in the same time. Increasing the value of power factor (PF) by selecting the suitable process parameters during machining is also recognized as a potential green machining strategy [17]. Also, it was noticed that in most of the research related to energy consumption for milling the geometry of the cutting tool was rarely used as the input parameters whereas, the geometrical features were used as input parameters in turning operations [3, 18, 19].

Another important problem faced by the machinists while achieving the higher production rates using the higher cutting speed, is the heat generation and the subsequent rise in the temperatures, which is detrimental to both the tool life and the surface quality. The energy used for metal cutting mostly gets converted into heat, which increases the temperatures in the machining zones [20, 21]. There are mainly three regions in which the heat generation occurs during the metal cutting processes; along the shearing plane due to plastic deformation of the metal; at line of contact between the tool and workpiece because of friction and at tool flank face because of the friction between the flank face and the machined surface. Beside the process parameters like cutting speed, feed, and depth of cut, the cutting temperature also depends on specific energy requirement, ductility, thermal conductivity, thermal diffusivity of the work material and tool geometry [22].

In the last few years, the researchers have started focusing on the reduction in the cutting temperatures during the machining processes. Tamilarasan et al. [23], formulated a multi objective optimization problem for the response variables like cutting zone temperature, tool wear and MRR. The model adequacy was confirmed through analysis of variance (ANOVA) and evolutionary algorithms like Genetic Algorithm (GA) and Simulated Annealing (SA) were used for optimization. Tamilsaran et al. [24, 25] also carried out multi objective optimization of workpiece surface temperature, cutting forces and sound pressure level for the tool steel material, using the work material hardness, nose radius, feed per tooth, radial and axial depth of cut as the input variables. The most influential parameter was feed rate, then, workpiece hardness and depth of cut. Multi objective GA was used by Hazza et al. [26] for minimization of the cutting temperature and surface roughness during end milling of AISI H 13 steel, using cutting speed, feed, and depth of cut as input variables and RSM for design of the experiments. The optimum values of cutting speed, feed and depth of cut were found to be 263 m/min, 0.07 mm/tooth and 0.11 mm respectively. The cutting temperature was found to be dependent on many factors like tool material, work piece material, process parameters like cutting speed, feed, and depth of cut.

The research of Le Coz et al. [27], Li et al. [28], Lazoglu et al. [29], highlights the importance of tool geometry for controlling the cutting temperatures, but the geometrical parameters as input variables were rarely used for the modelling of the temperatures. The energy consumption, temperature, cutting forces and induced stresses are affected by the geometrical features of the milling tool [30]. During energy and temperature related studies for milling; the cutting tool geometry is occasionally considered as an input parameter. It was noticed that the controllable machining parameters like cutting speed, feed rate and depth of cut are affecting the heat generation, energy consumption as well the surface quality. So, the selection of such parameters is vital in order to improve the overall performance of the machining processes. This selection is normally dependant on the recommendations in specialized handbooks along with the experience of the process engineers [7], but it fails to give the optimal values [3]. So, it is required to find the optimum values of the process parameters.

As compared to turning tools the end mill cutters are having many additional features which makes its geometry more complicated and so, to study the effect of such additional parameters is more important. In order to ensure smooth cutting action, in milling, the teeth are normally helical which allows engagement of more than one tooth and makes cutting smoother resulting in better finish [31]. Helix angle is the angle between a plane passing through the cutter axis and a tangent to the helix. The cutting tool's helix angle was not considered as a process parameter during the studies related to energy consumption in milling but its effect on cutting temperature rise was studied. Researchers have used the helix angle as input factor in other studies like Sivasakthivel et al.[32, 33, 34, 35] in modelling of vibration amplitude, tool wear, cutting forces and surface roughness; Hrikova et al.[36] and Tsao [37] for surface roughness; Kalidas et al. [38, 39] for surface roughness and tool wear. The variation in helix angle causing variation in machining performance, mainly regarding the energy consumption and heat generation, have not been discovered much. So, it is decided to include helix angle of the milling cutter as a input parameters for the current work, along with the controllable machining parameters like spindle speed, feed rate, axial depth of cut, radial depth of cut.

The literature review reveals that, beside the energy consumption; the energy efficiency and power factor are also important response parameters as they have direct influence on sustainability of machining. In the studies related to milling operation, these two response parameters were overlooked in the previous researches. The appropriate selection of machining parameters and tool geometry is needed in order to evaluate trade-offs between energy, heat generation and cutting quality and for this multi objective optimization problems needs to be formulated. Thus, in the current work, five objectives are considered; simultaneous minimization of the total energy consumption during machining (TECM), workpiece surface temperature rise (T) and surface roughness (Ra) and maximization of the energy efficiency (EE) and power

**Fig. 1** AMS milling machine



**Fig. 2** Sample workpieces of medium carbon steel (EN 8)

factor (PF). The response surface methodology was used for developing the mathematical models which were used as the input for the optimization. The direct and interaction effects of the input parameters on the response parameters were studied and discussed in details.

The inclusion of helix angle as an input factor and, using energy efficiency and power factor as output parameters are the major highlights of this work. This work also evaluates the trade-offs between energy, heat generation and cutting quality. Also, under different manufacturing circumstances different importance is given for energy consumption, cutting temperatures and surface roughness, so here, the multi objective optimization was carried out for three different situations by using desirability approach. Firstly, the energy parameters and surface quality was considered; in second situation only the workpiece surface temperature and surface roughness were the targets; and in third situation all the responses were considered for the multi objective optimization.

## 2 Experimental details

### 2.1 Workpiece, cutting tool, and machine tool description

The experiments were conducted on AMS make (model tool room) vertical, 3 axes CNC milling machining centre

(Fig. 1) having maximum spindle speed of 6000 rpm and 7.5 kW drive motor. The machining centre was a general purpose, compact, flexible, productive, robust, and high precision machine. The work table size of machine was 330 × 500 mm with XYZ travels of 300 mm × 250 mm × 250 mm. The work piece was placed in the machining centre using a machine vice and the cutting parameters were set according to the design of experiments.

The workpiece material selected for the experimentation was EN 8. It is a widely used medium carbon steel suitable for the all-general engineering applications requiring a higher strength than mild steel. It has good tensile strength and is often used in applications such as: general-purpose axles, shafts, gears, bolts and studs, spindles, automotive and general engineering components like stressed pins keys etc. The properties for EN 8 are listed in Table 1.

The test specimens were machined to a size of 150 mm length and 25 mm × 25 mm cross section from square bar (Fig. 2). In order to eliminate the rust and hardened top layer from the surface and to reduce effects of non-homogeneity on the experimental results; a pre-cut of 1 mm depth was performed on each workpiece prior to actual milling using different cutting tools. Solid uncoated tungsten carbide end mill cutters of 12 mm diameter (Fig. 3) were used for the experiments. Eight end mill cutters with five different helix angles cut on both the ends of the cutters were utilized. These tools were specially designed and manufactured by a local

**Table 1** Properties of EN 8

| Tensile strength (MPa) | Yield strength (MPa) | Elongation % | Hardness HBW | Specific heat J/kg K | Density kg/m$^3$ | Thermal conductivity, W/m K |
|---|---|---|---|---|---|---|
| 585.24 | 506.37 | 22.19 | 170–172 | 500 | 7850 | 46 |

**Fig. 3** END mill Cutter

**Table 2** Specifications of the end mill cutters

| (i)   | Number of flutes                      | 4                        |
|-------|---------------------------------------|--------------------------|
| (ii)  | Diameter of cutter                    | 12 mm                    |
| (iii) | Flute length                          | 30 mm                    |
| (iv)  | Rake angle                            | 7°                       |
| (v)   | Primary and secondary relief angles   | 9 and 18°                |
| (vi)  | Dish angle                            | 2°                       |
| (vii) | Helix angle                           | 10°, 20°, 30°, 40°, 50°  |

leading tool manufacturer. The specifications of the end mill cutters are as shown in Table 2.

## 2.2 Measuring instruments

HIOKI make, 3-Phase 4-Wire portable clamp on power quality analyzer PQ 3197 (basic accuracy: for active power, voltage and current: $\pm 0.3\%$) was used for the measurement of the energy consumption and power factor. This portable power quality analyser was the best-in-class power measuring instrument with a high degree of precision and accuracy. It was a portable power quality analyzer for monitoring and recording power supply anomalies, allowing their causes to be quickly investigated. The power analyser was connected to the main electric supply of the CNC milling machine. Figure 4, shows the power quality analyser and connection made in electric control panel of milling machine.

The rise in workpiece surface temperature (T) was recorded with the help of non-contact type infrared (IR) thermometer (HTC Make, Model IRX-67, least count 0.1 °C) equipped with smart sight laser system. The optical sensor can emit, reflect, and transmit energy, which is collected and focused on a detector, then translate it into the temperature reading by the electronics systems and displayed on the LCD screen. The smart sight laser system was used for aiming the target. The thermometer needs to be mounted as close as possible from the target, this was attained by using a specially designed holder for the thermometer.

Figure 5 shows the position of the thermometer with respect to the work piece. The surface roughness was



**a) Power quality analyser**
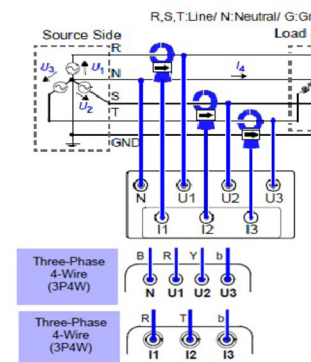


**b) Electrical connections in control panel of milling machine**

**Fig. 4** **a** Power quality analyser **b** Electrical connections in control panel of milling machine



**Fig. 5** Non-contact type thermometer

measured (Fig. 6) using SURFCOM 130A (Straightness accuracy- 0.3 m/50 mm) at the metrology lab of Nashik Engineering Cluster, Nashik, MS, India.

## 2.3 Design of experiment

After selecting the material, machine and cutting tool and measuring devices, machining experiments were conducted as per the scheme of runs determined by central composite design (CCD) used in response surface methodology (RSM) for design of experiments (DoE). The use the DoE gives conclusive results with reduced efforts, cost, and time. There are

**Fig. 6** Setup for surface roughness measurement

three major types of design of experiments methods; factorial DoE, RSM and Taguchi method. In the comparative studies[40, 19] the RSM was noticed to be better than Taguchi approach as it enables the experimenters to study the direct as well as interaction effects of the parameters and it also has got better visualization tools. RSM is useful for modelling and statistical analysis of the response parameters which are affected by a greater number of variables and responses [15]. It is usually used for developing the mathematical models for the response variables and to find out the influencing input variables and interactions [41]. For most RSM studies, central composite design (CCD) method which is a special case of factorial designs often used for design of the experiments. CCD needs five levels of each factor: $-\alpha$, $-1$, $0$, $1$, and $+\alpha$. The selected design consists of 32 experiments. This central composite rotatable design (CCRD) is having five factor and five levels for each factor. This CCRD consists of ½ replication of $2^5 (= 16)$ factorial design points, six centre points and ten-star points [42]. As it is a rotatable design, to maintain rotatability, the value of $\alpha$ depends upon the number of experimental runs in the factorial portion of the central composite design, $\alpha$ becomes, $2^{(k-1)/4}$ Where k = number of factors. As total number of parameters are five, $\alpha = 2$. The centre point was replicated to provide a measure of experimental error and hence while using second order rotatable designs no replications were needed in order to find the mean square error.

The selection of machining input process parameters was made by taking into consideration the capacity of the machine tool, tool manufacturer's recommendations and recommendations in the literature. Spindle speed (N), feed rate (F), Radial depth of cut (Y), axial depth of cut (Z) and helix angle (H) were the input process parameters chosen for the research. The initial levels of cutting speed and feed rate were decided using the recommendation of Li et al. [7] and Kadirgama et al. [10]. The method adopted by Patel et al. [43] was used for the calculations of the other levels. The average cutting speed was taken as 100 m/min and feed per tooth was taken as 0.025 mm/toot. For the average cutting speed 100 m/min and for a tool diameter of 12 mm; the corresponding spindle speed was calculated as 2500 rpm and feed per minute as 250 m/min and both were varied by $+/-20\%$.

The axial and radial depth of cut values were decided using recommendation of the tool manufacurer and through the results of the pilot experimentations. The helix angle range was decided using recommendation of the tool manufacurer and the using the recommendations in literature by Sivasakthivel et al. [44] and Vikas et al. [30]. Table 3 shows the machining parameters and the levels for each parameter.

Table 4 shows the scheme of the experimentation with the uncoated factors values.

## 2.4 Measured responses

The experimentation was carried out using the scheme of the experimentation as shown in Table 4 and the measurement systems were employed for measuring and recording of the data. The cycle time, power consumption during the cycle with and without workpiece, workpiece surface temperatures were recorded at the time of experimentation. The details of the calculation methodology is explained below.

Using the power quality analyser PQ 3197; the value of power consumed when the actual cutting of material was taking place by the machine (PCM in Watt) was recorded. Similarly, the power consumed by the machine during air cutting (no workpiece) was also recorded (PCA in Watt). The difference in these two power readings was called as power consumed for cutting (PC). The power factor during machining cycle and cycle time in seconds were recorded simultaneously. The total energy consumed for machining (TECM) was the product of PCM and cycle time and was in Joules. The product of PC and cycle time was termed as cutting energy (CE). The energy efficiency (EE) was the ratio of CE and TECM expressed in percentage.

$$EE\ (\%) = \frac{CE}{TECM} \times 100 \tag{1}$$

The initial and maximum temperatures were recorded during machining, and the difference between them was referred as temperature rise. The surface roughness of all the samples was measured using SURFCOM 130A after the experimentation. Surface roughness was measured at three places on the machined surface and average value was taken in order to reduce error in measurements. The results obtained from experimentation and calculations, are summarised in the Table 5.

## 3 Results and discussions

### 3.1 Response surface methodology

The first stage for the RSM is to find out a suitable function which represents the relationship between input and output variable. Generally, two important models are used in RSM.

**Table 3** Level of input process parameters for EN8

| Levels | Lowest | Low | Centre | High | Highest |
|---|---|---|---|---|---|
| Coding | $-\alpha$ | $-1$ | 0 | $+1$ | $+\alpha$ |
| Spindle speed, N, rpm | 1500 | 2000 | 2500 | 3000 | 3500 |
| Feed, F mm/min | 150 | 200 | 250 | 300 | 350 |
| Radial depth of cut, Y mm | 2 | 40 | 6 | 8 | 10 |
| Axial depth of cut, X mm | 0.5 | 1 | 1.5 | 2 | 2.5 |
| Helix angle, H ° | 10 | 20 | 30 | 40 | 50 |

**Table 4** Uncoated factors values for experiments

| Std order | Spindle speed, N, rpm | Feed F, mm/min | Radial depth of cut, Y, mm | Axial depth of cut Z, mm | Helix angle H, ° | Std order | Spindle Speed, N, rpm | Feed F, mm/min | Radial depth of cut, Y, mm | Axial depth of cut Z, mm | Helix angle H, ° |
|---|---|---|---|---|---|---|---|---|---|---|---|
| 1 | 2000 | 200 | 4 | 1 | 40 | 17 | 1500 | 250 | 6 | 1.5 | 30 |
| 2 | 3000 | 200 | 4 | 1 | 20 | 18 | 3500 | 250 | 6 | 1.5 | 30 |
| 3 | 2000 | 300 | 4 | 1 | 20 | 19 | 2500 | 150 | 6 | 1.5 | 30 |
| 4 | 3000 | 300 | 4 | 1 | 40 | 20 | 2500 | 350 | 6 | 1.5 | 30 |
| 5 | 2000 | 200 | 8 | 1 | 20 | 21 | 2500 | 250 | 2 | 1.5 | 30 |
| 6 | 3000 | 200 | 8 | 1 | 40 | 22 | 2500 | 250 | 10 | 1.5 | 30 |
| 7 | 2000 | 300 | 8 | 1 | 40 | 23 | 2500 | 250 | 6 | 0.5 | 30 |
| 8 | 3000 | 300 | 8 | 1 | 20 | 24 | 2500 | 250 | 6 | 2.5 | 30 |
| 9 | 2000 | 200 | 4 | 2 | 20 | 25 | 2500 | 250 | 6 | 1.5 | 10 |
| 10 | 3000 | 200 | 4 | 2 | 40 | 26 | 2500 | 250 | 6 | 1.5 | 50 |
| 11 | 2000 | 300 | 4 | 2 | 40 | 27 | 2500 | 250 | 6 | 1.5 | 30 |
| 12 | 3000 | 300 | 4 | 2 | 20 | 28 | 2500 | 250 | 6 | 1.5 | 30 |
| 13 | 2000 | 200 | 8 | 2 | 40 | 29 | 2500 | 250 | 6 | 1.5 | 30 |
| 14 | 3000 | 200 | 8 | 2 | 20 | 30 | 2500 | 250 | 6 | 1.5 | 30 |
| 15 | 2000 | 300 | 8 | 2 | 20 | 31 | 2500 | 250 | 6 | 1.5 | 30 |
| 16 | 3000 | 300 | 8 | 2 | 40 | 32 | 2500 | 250 | 6 | 1.5 | 30 |

1. First-degree model (d = 1).
2. Second-degree model (d = 2).

If the response of the system under consideration can be sufficiently modelled using a linear function of the input variables, a first-order model is used. Mathematically, this can be expressed as Eq. (2);

$$y = bo + b_1X_1 + b_2X_2 + \ldots b_iX_i + e \qquad (2)$$

For more complex response a second-order model is used. The second order model is given by Eq. (3);

$$y = b_o + \sum_{i=1}^{k} b_{ii}X_i + \sum_{i=1}^{k} b_{ii}X_i^2 + \sum_{i<j} b_{ij}X_iX_j + e \qquad (3)$$

where, the term "e" represents the error or noise in the response y and b's are the regression coefficients to be calculated using the least square technique [45]. The least square method is used to determine the parameters in the models. In present study, statistical analysis is done and models are developed for aal the responses in terms of process parameters. The adequacy of the model was confirmed using analysis of variance (ANOVA). The models generation, the direct and interaction effects of process parameters on the response variables are analysed and discussed in the subsequent sections.

## 3.2 Model generation for total energy consumption

The results of the experimentation were used for the generation of the second-degree polynomial empirical models. Least square technique was used for the estimation of the regression coefficients. Analysis of variance was carried to find the effective parameters in the developed model and the

**Table 5** Experimental results for EN8

| Std order | Cycle time, s | PCM, W | PCA, W | PC, W | TECM, J | EE % | PF | T °C | Ra, μm |
|---|---|---|---|---|---|---|---|---|---|
| 1 | 53 | 538 | 495 | 43 | 28,514 | 7.99 | 0.785 | 20.2 | 0.319 |
| 2 | 53 | 561 | 501 | 60 | 29,733 | 10.70 | 0.791 | 23.2 | 0.220 |
| 3 | 37 | 546 | 488 | 58 | 20,202 | 10.62 | 0.788 | 32.2 | 0.321 |
| 4 | 37 | 594 | 519 | 75 | 21,978 | 12.63 | 0.804 | 19.6 | 0.245 |
| 5 | 53 | 560 | 482 | 78 | 29,680 | 13.93 | 0.794 | 50.4 | 0.373 |
| 6 | 53 | 590 | 502 | 88 | 31,270 | 14.92 | 0.809 | 32.6 | 0.310 |
| 7 | 37 | 609 | 496 | 113 | 22,533 | 18.56 | 0.811 | 42.6 | 0.387 |
| 8 | 37 | 613 | 517 | 96 | 22,681 | 15.66 | 0.808 | 46.8 | 0.379 |
| 9 | 53 | 568 | 476 | 92 | 30,104 | 16.20 | 0.795 | 37.8 | 0.334 |
| 10 | 53 | 649 | 504 | 145 | 34,397 | 22.34 | 0.831 | 63.8 | 0.420 |
| 11 | 37 | 621 | 493 | 128 | 22,977 | 20.61 | 0.821 | 47.8 | 0.532 |
| 12 | 37 | 687 | 583 | 104 | 25,419 | 15.14 | 0.845 | 41 | 1.273 |
| 13 | 53 | 691 | 477 | 214 | 36,623 | 30.97 | 0.856 | 87.4 | 0.430 |
| 14 | 53 | 675 | 503 | 172 | 35,775 | 25.48 | 0.834 | 70.6 | 0.942 |
| 15 | 37 | 773 | 537 | 236 | 28,601 | 30.53 | 0.862 | 73 | 1.130 |
| 16 | 37 | 823 | 518 | 305 | 30,451 | 37.06 | 0.865 | 109.4 | 0.959 |
| 17 | 43 | 638 | 527 | 111 | 27,434 | 17.40 | 0.834 | 51.4 | 0.290 |
| 18 | 43 | 723 | 579 | 144 | 31,089 | 19.92 | 0.848 | 39.6 | 0.140 |
| 19 | 69 | 603 | 523 | 80 | 41,607 | 13.27 | 0.818 | 39.4 | 0.088 |
| 20 | 33 | 639 | 535 | 104 | 21,087 | 16.28 | 0.815 | 35.6 | 0.369 |
| 21 | 43 | 579 | 541 | 38 | 24,897 | 6.56 | 0.811 | 17 | 0.456 |
| 22 | 43 | 704 | 527 | 177 | 30,272 | 25.14 | 0.84 | 60.8 | 0.347 |
| 23 | 43 | 558 | 533 | 25 | 23,994 | 4.48 | 0.768 | 14.2 | 0.490 |
| 24 | 43 | 736 | 518 | 218 | 31,648 | 29.62 | 0.851 | 93 | 1.150 |
| 25 | 43 | 635 | 513 | 122 | 27,305 | 19.21 | 0.815 | 41.4 | 0.590 |
| 26 | 43 | 708 | 511 | 197 | 30,444 | 27.82 | 0.846 | 73 | 0.488 |
| 27 | 43 | 607 | 523 | 84 | 26,101 | 13.84 | 0.814 | 40.2 | 0.248 |
| 28 | 43 | 617 | 527 | 90 | 26,531 | 14.59 | 0.798 | 39.6 | 0.303 |
| 29 | 43 | 592 | 518 | 74 | 25,456 | 12.50 | 0.797 | 40.2 | 0.311 |
| 30 | 43 | 580 | 515 | 65 | 24,940 | 11.21 | 0.802 | 41.2 | 0.239 |
| 31 | 43 | 573 | 515 | 58 | 24,639 | 10.12 | 0.802 | 42.6 | 0.116 |
| 32 | 43 | 590 | 515 | 75 | 25,370 | 12.71 | 0.797 | 31.2 | 0.238 |

non-effective parameters were removed by backward elimination method [15, 42]. The model significance was checked using the F- values and *p*- values. The residual plots were used for checking the fitness of the model. Finally, the analysis of the effects of the input process parameters on the response variables was carried out using the main effects plots and surface plots.

Table 6 shows the ANOVA results for the TECM along with the model summary.

The higher value of the coefficient of determination, R-sq for this model (95.05%) shows that the experimental data was well described by this model. The R-sq value for the model was close to the adjusted coefficient of determination value of the model (R-sq (adj) = 93.03%). Also, the value of R-sq (pred) was in reasonable agreement with the R-sq (adj) value. The model F-value of 46.97 implies that model was significant and there was very little possibility that model F-Value this large could occur due to noise. *P* value of the model was less than 0.05 which also indicates model was fitting all the design points well. The F value for lack of fit is 3.92 and *p* value was 0.069 indicates insignificant lack of fit. The second order model in uncoded units is as shown in Eq. (4).

$$TECM = 85532 - 10.32N - 309.3F$$
$$- 471Y - 384Z - 248H$$

**Table 6** ANOVA results for TECM

| Source | DF | Seq SS | Adj SS | Adj MS | F-value | P-value |
|---|---|---|---|---|---|---|
| Model | 9 | 687,718,940 | 687,718,940 | 76,413,216 | 46.97 | 0.000 |
| Linear | 5 | 627,641,950 | 627,641,950 | 125,528,390 | 77.16 | 0.000 |
| N | 1 | 16,302,017 | 16,302,017 | 16,302,017 | 10.02 | 0.004 |
| F | 1 | 436,002,602 | 436,002,602 | 436,002,602 | 267.99 | 0.000 |
| Y | 1 | 51,158,400 | 51,158,400 | 51,158,400 | 31.44 | 0.000 |
| Z | 1 | 117,324,504 | 117,324,504 | 117,324,504 | 72.11 | 0.000 |
| H | 1 | 6,854,428 | 6,854,428 | 6,854,428 | 4.21 | 0.052 |
| Square | 3 | 49,811,374 | 49,811,374 | 16,603,791 | 10.21 | 0.000 |
| N*N | 1 | 7,218,689 | 10,649,539 | 10,649,539 | 6.55 | 0.018 |
| F*F | 1 | 35,107,148 | 37,276,160 | 37,276,160 | 22.91 | 0.000 |
| H*H | 1 | 7,485,537 | 7,485,537 | 7,485,537 | 4.6 | 0.043 |
| 2-way interaction | 1 | 10,265,616 | 10,265,616 | 10,265,616 | 6.31 | 0.020 |
| Y*Z | 1 | 10,265,616 | 10,265,616 | 10,265,616 | 6.31 | 0.020 |
| Error | 22 | 35,792,840 | 35,792,840 | 1,626,947 | | |
| Lack-of-fit | 17 | 33,295,149 | 33,295,149 | 1,958,538 | 3.92 | 0.069 |
| Pure error | 5 | 2,497,691 | 2,497,691 | 499,538 | | |
| Total | 31 | 723,511,780 | | | | |

| S | R-sq | R-sq(adj) | Press | R-sq(pred) |
|---|---|---|---|---|
| Model summary | | | | |
| 1275.52 | 95.05% | 93.03% | 96,653,370 | 86.64% |

$$+ 0.002395 N*N + 0.4480 F*F$$
$$+ 5.02 H*H + 801\, Y \tag{4}$$

The model adequacy was examined using the residuals. The residual means the differences between the observed value and the predicted value of the response. Figure 7 shows the residual plot for TECM for checking the model adequacy.

In the normal probability plots the residuals were following a straight line and in the versus fit plot the residuals were randomly scattered about the zero line. For an adequate model, the points on the normal probability plots of the residuals should form a straight line. Figure 7 also illustrates that the residuals were not showing a particular trend and the errors were distributed normally. The residual versus the predicted response plot also shows that there is no noticeable pattern and unusual structure. The nature of the histogram and residuals versus order graphs shows that fitted model values were closer to the experimental values.

Figure 8, shows the effect of various input parameters on TECM. The feed rate was the most significant parameter affecting the TECM followed by axial depth of cut. It was noticed that the TECM reduces as the feed rate increases. As the feed rate increases the cycle time gets reduced as axis of the motors needs to move faster, which results in to reduction in energy consumed. Similar observations were made by Negrete et al. [46], Bilga et al. [3], Mativenga et al. [47].

The smaller spindle speed was also contributing to reduced energy [18, 19, 48]. The smaller values of radial as well as axial depth of cut were resulting in to smaller energy consumption because as the depth of cut increases, more forces are needed to remove the material for the harder materials like EN8 as the contact area between the workpiece and the tool increases and thus, more power is needed for cutting of the material [3, 49]. The similar results were obtained by Yusoff et al. [50] during milling of cast iron. The helix angle was not having much significant effect on the energy consumption, but still helix angle around 30° was resulting in minimum energy consumption. Like the findings of Altintas et al. [51], low spindle speed and higher feed rates was resulting in to lower energy consumption.

The surface plot for effect of axial and radial depth of cut on TECM (Fig. 9) demonstrates that the combination of higher radial and axial depth of cut was resulting in to higher energy consumption as more material removal needs more energy consumption. The increase in the axial depth of cut at larger value of the radial depth was resulting in to more energy consumption. The effect of axial depth of cut was more significant as compared to radial depth of cut, so by controlling axial depth of cut energy consumption can be reduced.
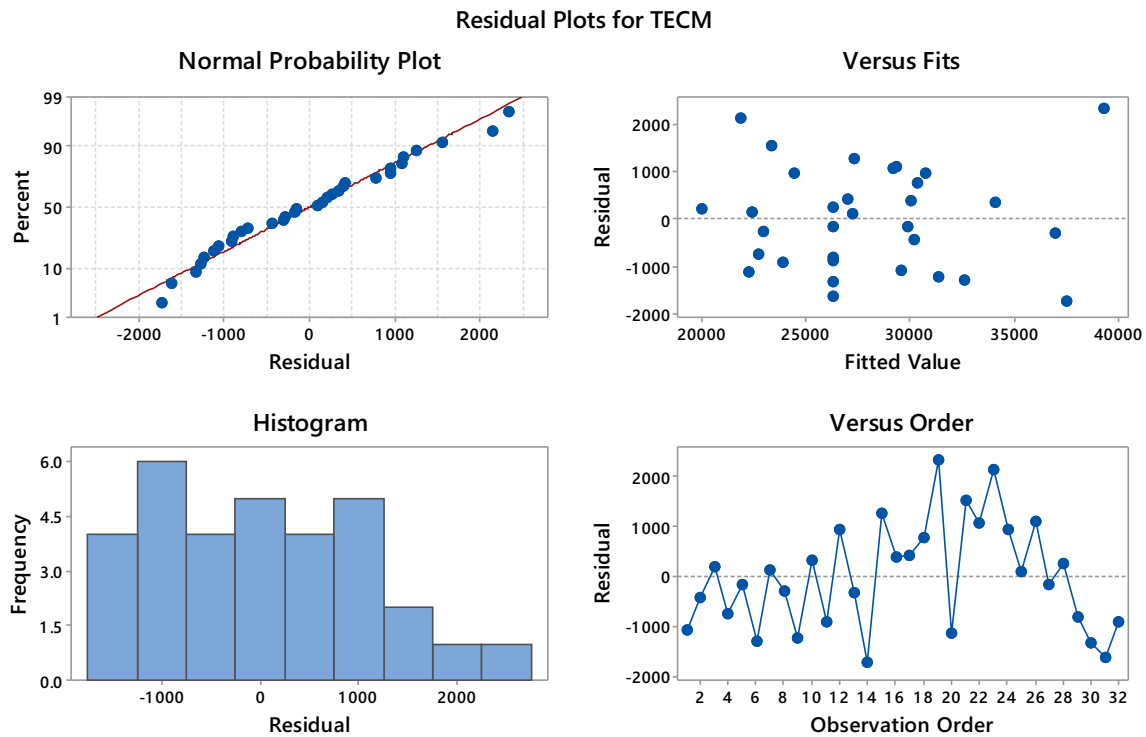
**Residual Plots for TECM**

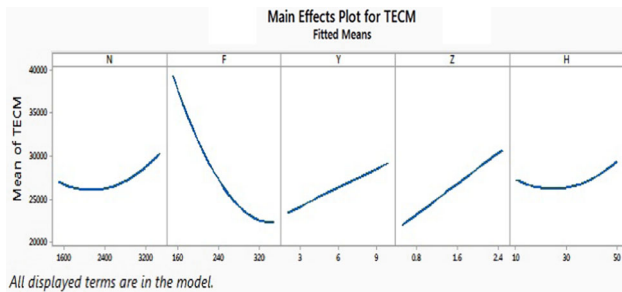

**Fig. 7** Residual plots for TECM



**Fig. 8** Main effects plot for TECM
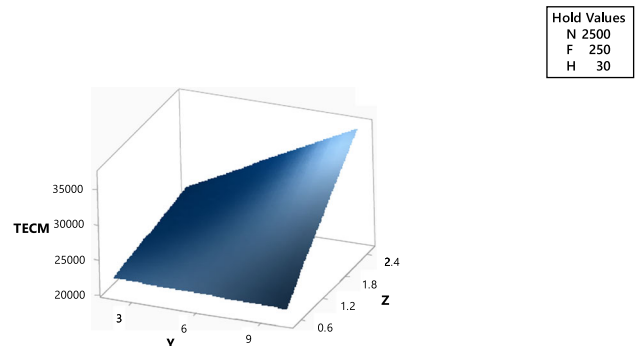
## 4 Model generation for energy efficiency

Like the previous analysis, the ANOVA was used to find out the effective parameters in the mathematical model and the non-effective parameters were removed by backward elimination method. Table 7 shows the ANOVA results along with the model summary. The second order model in uncoded units is as shown in Eq. (5),

$$EE = 112.3 - 0.03355N - 0.1350F - 5.05Y$$
$$- 19.27Z - 2.222H + 0.000006N * N$$
$$+ 0.000200F * F + 0.1926Y * Y$$
$$+ 4.278Z * Z + 0.02687H * H$$
$$+ 0.000164N * H + 0.00921F * Y$$



**Fig. 9** Effect of axial and radial depth of cut on TECM

$$+ 1.789Y * Z + 0.2557Z * H \qquad (5)$$

Here, higher R-sq value (98.58%) was observed and it was found to be close to the adjusted coefficient of determination value of the model (R-sq (adj) = 97.40%). Also, the value of R-sq (pred) was in reasonable agreement with the R-sq (adj) value. The F-value of was 84.09, it means that model was significant and there was a very slight chance that model F-Value this high could occur due to noise. *P* value of the model was less than 0.05 which was also an indicator of model fitting all the design points well. The F value for lack of fit was 0.4 and *p* value was 0.910 signifies insignificant lack of fit. Figure 10 shows the residual plots for EE for

**Table 7** ANOVA results for EE

| Source | DF | Seq SS | Adj SS | Adj MS | F-value | P-value |
|---|---|---|---|---|---|---|
| Model | 14 | 1836.02 | 1836.02 | 131.144 | 84.09 | 0.000 |
| Linear | 5 | 1454.88 | 1454.88 | 290.975 | 186.57 | 0.000 |
| N | 1 | 3.8 | 3.8 | 3.799 | 2.44 | 0.137 |
| F | 1 | 24.6 | 24.6 | 24.603 | 15.78 | 0.001 |
| Y | 1 | 486.29 | 486.29 | 486.292 | 311.8 | 0.000 |
| Z | 1 | 859.36 | 859.36 | 859.36 | 551.01 | 0.000 |
| H | 1 | 80.82 | 80.82 | 80.822 | 51.82 | 0.000 |
| Square | 5 | 279.44 | 279.44 | 55.889 | 35.84 | 0.000 |
| N*N | 1 | 38.74 | 63.52 | 63.518 | 40.73 | 0.000 |
| F*F | 1 | 0.93 | 7.33 | 7.332 | 4.7 | 0.045 |
| Y*Y | 1 | 6.88 | 17.4 | 17.404 | 11.16 | 0.004 |
| Z*Z | 1 | 21.13 | 33.56 | 33.56 | 21.52 | 0.000 |
| H*H | 1 | 211.76 | 211.76 | 211.758 | 135.78 | 0.000 |
| 2-way interaction | 4 | 101.7 | 101.7 | 25.426 | 16.3 | 0.000 |
| N*H | 1 | 10.75 | 10.75 | 10.754 | 6.9 | 0.018 |
| F*Y | 1 | 13.58 | 13.58 | 13.577 | 8.71 | 0.009 |
| Y*Z | 1 | 51.23 | 51.23 | 51.225 | 32.85 | 0.000 |
| Z*H | 1 | 26.15 | 26.15 | 26.147 | 16.77 | 0.001 |
| Error | 17 | 26.51 | 26.51 | 1.56 | | |
| Lack-of-fit | 12 | 13 | 13 | 1.083 | 0.4 | 0.910 |
| Pure error | 5 | 13.52 | 13.52 | 2.703 | | |
| Total | 31 | 1862.54 | | | | |

| S | R-sq | R-sq (adj) | Press | R-sq(pred) |
|---|---|---|---|---|
| Model summary | | | | |
| 1.24884 | 98.58% | 97.40% | 78.4652 | 95.79% |

checking the model adequacy, in the normal probability plot the residuals were following a straight line and in the versus fit plot the residuals were randomly scattered about the zero line.

Figure 11 shows the main effects plot of various input parameters on EE. The EE was found to be increasing with the feed rate, axial depth of cut and radial depth of cut. The Effect of feed rate on EE was comparatively smaller. Similar observations was also reported by Bilga et al. [3] during CNC rough turning of EN 353 alloy steel. The higher value of EE was noticed for higher helix angle. So, higher energy efficiency during milling of EN 8 can be obtained with combination of higher depth of cut, feed rate, and helix angle. In the surface plot of effect of helix angle and spindle speed on EE (Fig. 12), the higher EE was observed at higher spindle speed with the tool with higher helix angle. The energy efficiency was proportional to the power consumed in cutting, PC [3]. It means, more power was required to cut the material with higher helix angle tool at higher spindle speed.

As shown in Figs. 13 and 14, the higher value of energy efficiency was obtained for high radial and axial depth of cut because for higher depth of cuts more power was required for the machining as the contact area between the workpiece and the tool increases which increases load on the electric motor [49] So, higher feed rate, and depths of cut were found to be improving the energy efficiency.

Figure 15 shows the effect of helix angle and axial depth of cut variation the energy efficiency. The highest value of EE was seen at the top right corner of the figure. It can be noticed that, the cutting process becomes more energy efficient with increase in both the helix angle and the axial depth of cut. Thus the combination of high depth of cut and higher helix angle was helpful for improvement in EE of the process.

## 4.1 Model generation for power factor

Analysis of variance was carried out to find out the effective parameters in the developed model and the non-effective parameters were removed by backward elimination method.
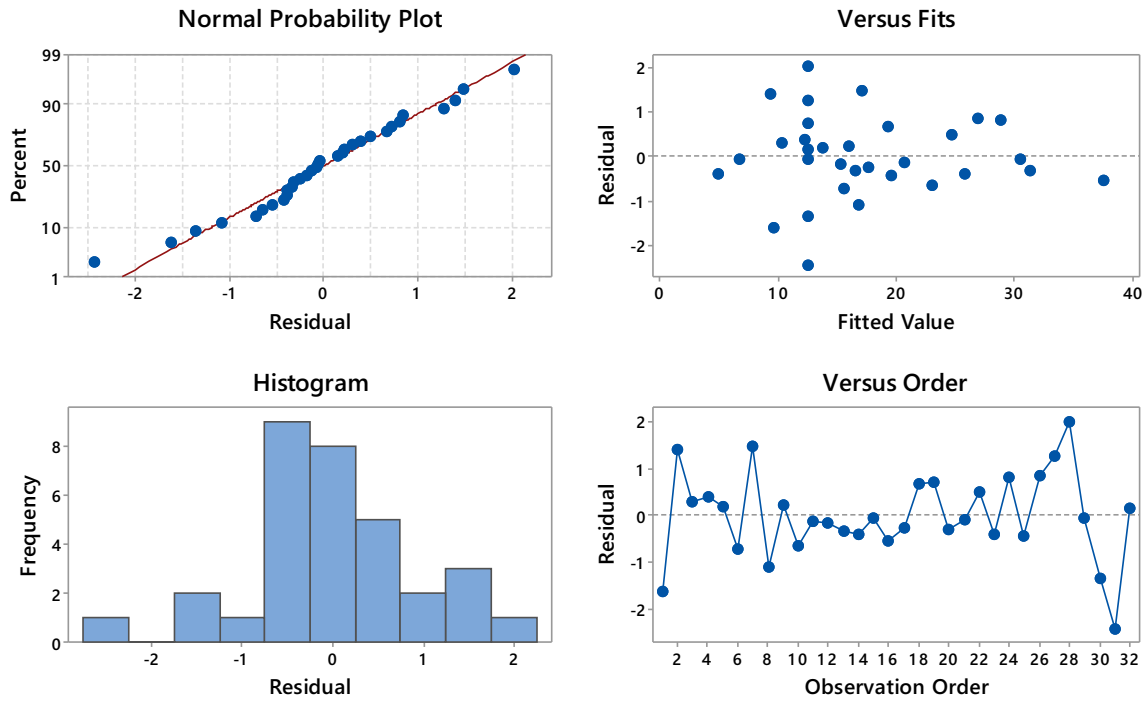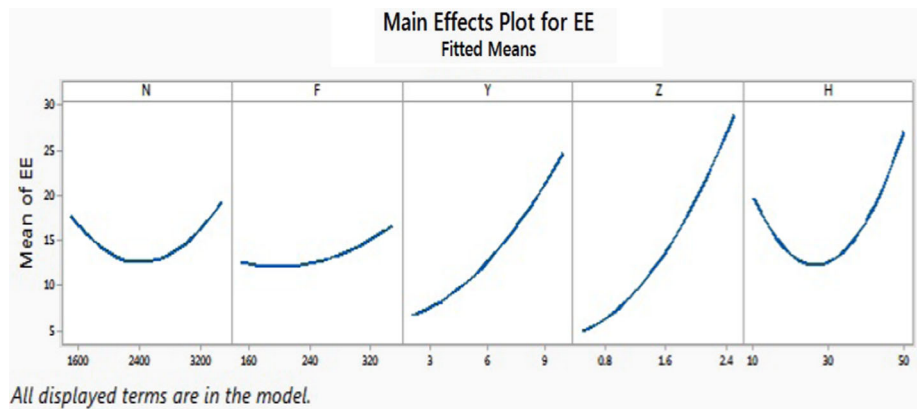
**Residual Plots for EE**

**Normal Probability Plot**

**Versus Fits**

**Histogram**

**Versus Order**

**Fig. 10** Residual plots for EE

**Fig. 11** Main effects plot of input parameters on EE

**Main Effects Plot for EE**
Fitted Means

All displayed terms are in the model.

**Surface Plot of EE vs H, N**

Hold Values
F 250
Y 6
Z 1.5
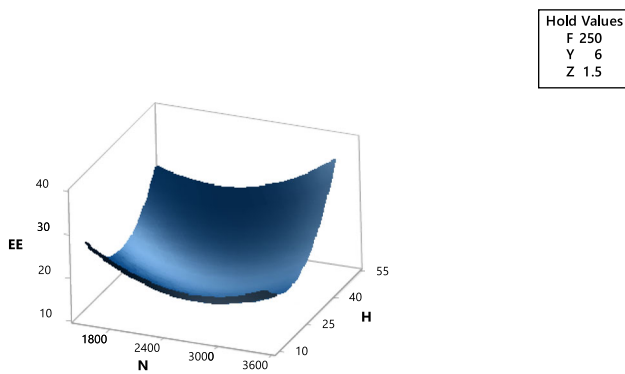
**Fig. 12** Effect of helix angle and spindle speed on EE

**Surface Plot of EE vs Y, F**

Hold Values
N 2500
Z 1.5
H 30
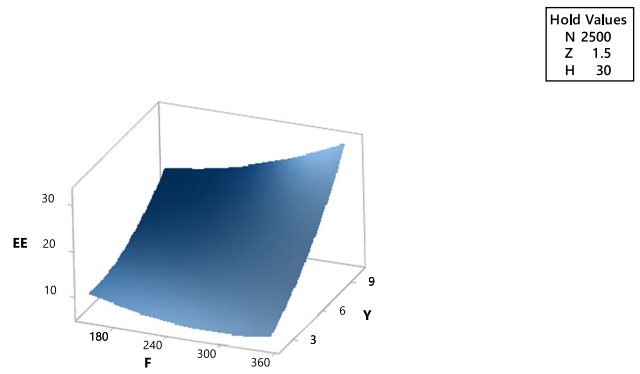
**Fig. 13** Effect of radial depth of cut and feed on EE

## Surface Plot of EE vs Z, Y
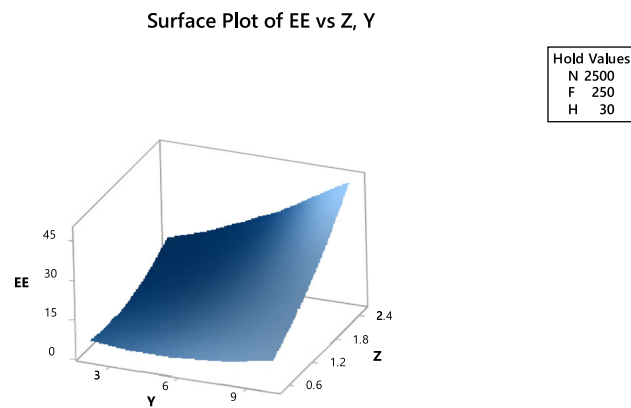


**Fig. 14** Effect of axial and radial depth of cut on EE

## Surface Plot of EE vs H, Z
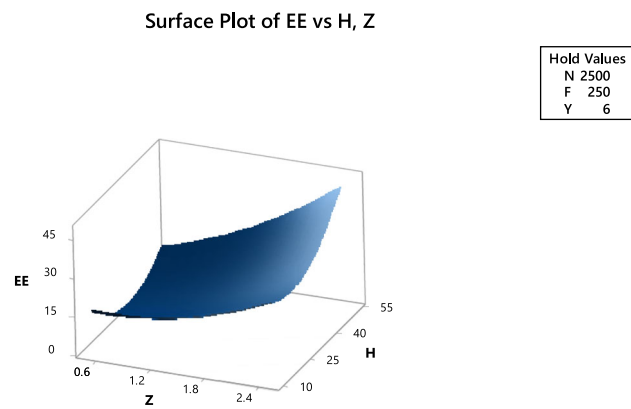


**Fig. 15** Effect of helix angle and axial depth of cut on EE

Table 8 shows the ANOVA results for the PF along with the model summary. The second order model in uncoded units is as shown in Eq. (6),

$$
\begin{aligned}
PF ={}& 0.8164 - 0.000110N + 0.000345F \\
& + 0.00100Y + 0.0138Z - 0.00030H \\
& + 0.000000N * N + 0.000933Y * Y \\
& + 0.000050H * H - 0.000006N * Y \\
& - 0.000009F * H + 0.00444Y * Z
\end{aligned}
\tag{6}
$$

This model has R-sq value = 91.98%; R-sq (adj) = 87.57% and R-sq (pred) 77.68%, which depict that the experimental data was well fitted by this model. The F-value of was 20.85, it means that model was significant and there was little chance that model F-Value this high could occur due to noise. *P* value of the model was less than 0.05 which was also an indicator of model fitting all the design points well. The F value and *p* value for lack of fit were 2.08 and 0.215 respectively, indicating insignificant lack of fit.

Figure 16 shows the residual plots for power factor in order to check the model adequacy, in the normal probability plot

the residuals were following a straight line and in the versus fit plot the at random spread of residuals was observed. The histogram and residuals versus order graphs also indicates that fitted model values were closer to the experimental values.

The main effects plot of the control parameters on power factor is shown in Fig. 17, the axial depth of cut was the most significant parameter followed by radial depth of cut and helix angle. The effects of spindle speed and feed rate were less significant. Higher axial and radial depths of cut were leading into higher power factor values. The similar results were reported by Bilga et al. [3]. The power factor is proportional to the active power drawn from the electrical drive motor. When the load on the drive motor increases, more power is required to overcome the load and this increases the power factor [52]. So, higher spindle speed, feed rate, and depth of cut which increases the load on motor results in to increase in the value of power factor.

The surface plot of the effects of spindle speed and radial depth of cut on PF is shown in Fig. 18. The highest value of PF was realized when the spindle speed was less and radial depth of cut was higher. Higher depth of cut increases load on the motor which results in to higher PF. However, the higher PF was also noticed at high spindle speed and less radial depth of cut combination. It can also be observed that, for the smaller radial depth of cut increase in the spindle speed beyond 2500 rpm suddenly increases the value of PF which indicated that for higher spindle speeds the lower radial depth needs to preferred in order to get better power factor values.

From Fig. 19, it can be observed that larger value of helix angle and smaller feed rate results in increase in the value of the power factor. The power factor was also seen to be higher for the combination of high feed with less helix angle. For less helix angle the PF increases steadily with increase in the feed rate and for higher helix tool as the feed rate increases the power factor reduces. The surface plot for radial and axial depth of cut (Fig. 20) illustrates that, the axial depth of cut was having more impact on PF, as compared to radial depth of cut. Higher PF was obtained at larger value of axial depth of cut. The PF was not getting affected much; if the radial depth of cut was increased keeping axial depth of cut smaller.

## 4.2 Model generation for workpiece surface temperature rise

Second order quadratic model was developed using the response surface method. Analysis of variance was carried to find out the effective parameters in the developed model and the non-effective parameters were removed by backward elimination method. Table 9 shows the ANOVA results for

**Table 8** ANOVA results for PF

| Source | DF | Seq SS | Adj SS | Adj MS | F-value | P-value |
|---|---|---|---|---|---|---|
| Model | 11 | 0.01736 | 0.01736 | 0.001578 | 20.85 | 0.000 |
| Linear | 5 | 0.0137 | 0.0137 | 0.00274 | 36.19 | 0.000 |
| N | 1 | 0.00044 | 0.00044 | 0.000442 | 5.84 | 0.025 |
| F | 1 | 0.00044 | 0.00044 | 0.000442 | 5.84 | 0.025 |
| Y | 1 | 0.00234 | 0.00234 | 0.00234 | 30.91 | 0.000 |
| Z | 1 | 0.0098 | 0.0098 | 0.009801 | 129.46 | 0.000 |
| H | 1 | 0.00067 | 0.00067 | 0.000672 | 8.88 | 0.007 |
| Square | 3 | 0.00256 | 0.00256 | 0.000853 | 11.26 | 0.000 |
| N*N | 1 | 0.00148 | 0.00172 | 0.001719 | 22.71 | 0.000 |
| Y*Y | 1 | 0.00034 | 0.00041 | 0.000414 | 5.46 | 0.030 |
| H*H | 1 | 0.00074 | 0.00074 | 0.000737 | 9.74 | 0.005 |
| 2-way interaction | 3 | 0.00111 | 0.00111 | 0.000369 | 4.88 | 0.011 |
| N*Y | 1 | 0.0005 | 0.0005 | 0.000495 | 6.54 | 0.019 |
| F*H | 1 | 0.0003 | 0.0003 | 0.000298 | 3.93 | 0.061 |
| Y*Z | 1 | 0.00032 | 0.00032 | 0.000315 | 4.16 | 0.055 |
| Error | 20 | 0.00151 | 0.00151 | 0.000076 | | |
| Lack-of-fit | 15 | 0.00131 | 0.00131 | 0.000087 | 2.08 | 0.215 |
| Pure error | 5 | 0.00021 | 0.00021 | 0.000042 | | |
| Total | 31 | 0.01888 | | | | |

| S | R-sq | R-sq (adj) | Press | R-sq (pred) | |
|---|---|---|---|---|---|
| Model summary | | | | | |
| 0.0087009 | 91.98% | 87.57% | 0.00421 | 77.68% | |

### Residual Plots for PF
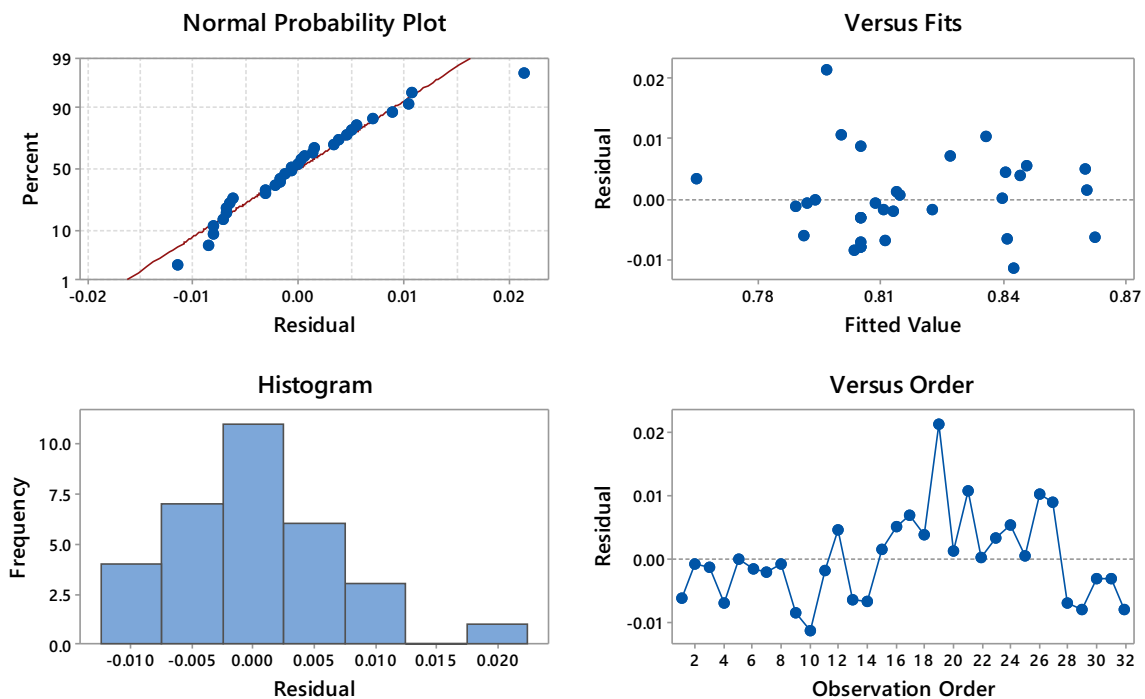


**Fig. 16** Residual plots for Power factor

**Fig. 17** Main effects plot for Power factor
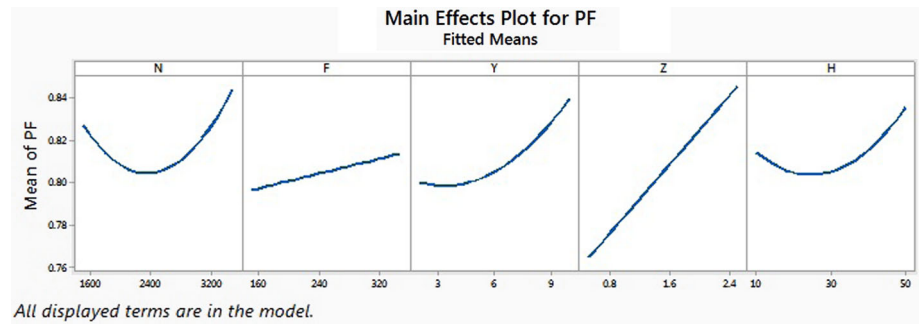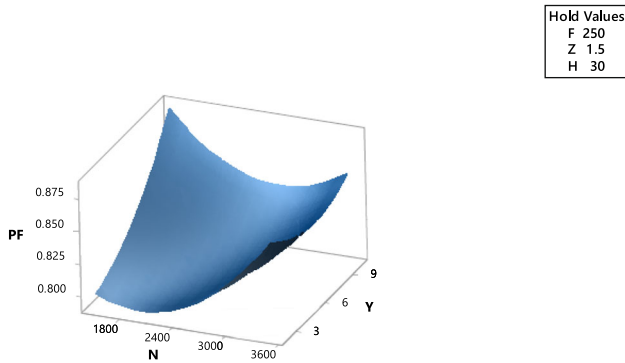


**Fig. 18** Effects of spindle speed and radial depth of cut on PF
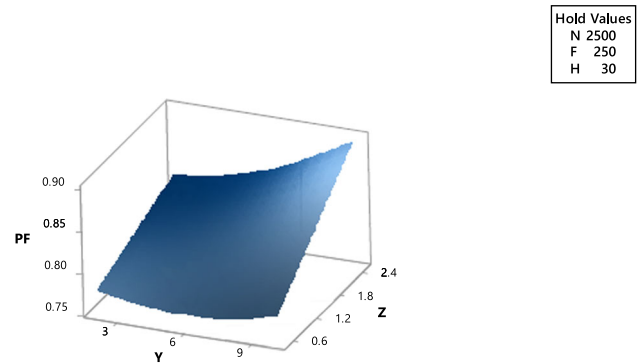


**Fig. 19** Effects of feed rate and helix angle on PF



**Fig. 20** Effects of radial and axial depth of cut on PF



the temperature rise along with the model summary. The second order model in uncoded units is as shown in Eq. (7),

$$
\begin{aligned}
T =\ & 264.3 - 0.0757N - 0.27Y - 123.9Z \\
& - 5.94H + 0.000007N*N + 15.52Z*Z \\
& + 0.0478H*H + 0.01550N*Z + 0.000490N*H \\
& + 4.55Y*Z + 1.545Z*H
\end{aligned} \tag{7}
$$

The R-sq value was 96.07% which explains that the experimental data was well fitted by this model. The R-sq value for the model was close to R-sq (adj). Also, the value of R-sq (pred) was in reasonable agreement with the R-sq (adj) value. The F-value of model was 44.45, it means that model is significant and there is very small chance that model F-Value this high could occur due to noise. *P* value of the model was less than 0.05 which was also an indicator of model fitting all the design points well. The F value for lack of fit was 2.13 and *p* value was 0.207 indicates insignificant lack of fit.

Figure 21, shows the residual plots for temperature rise in order to check the model adequacy, in the normal probability plot the residuals were following a straight line and in the versus fit plot the residuals were randomly scattered about the zero line. The histogram and residuals versus order graphs also indicates that fitted model values were closer to the experimental values.

The main effects plot for temperature rise is shown in Fig. 22. The most significant effect was of the axial depth of cut followed by radial depth of cut and helix angle. It was observed that the temperature rise increases with increase in both the axial and radial depths of cut. The increase of these depths of cut results in to increase in the contact area of the tool with the workpiece which results in more heat generation and higher temperature [53]. Feed rate and spindle speed were less significant for the temperature rise. The similar observations were reported by Kus et al. [54] and Gosai et al. [55] during turning of steel, and Patel et al. [56] during milling of mild steel. Slightly reducing trend in the

**Table 9** ANOVA results for the temperature rise

| Source | DF | Seq SS | Adj SS | Adj MS | F-value | P-value |
|---|---|---|---|---|---|---|
| Model | 11 | 14,752.3 | 14,752.3 | 1341.12 | 44.45 | 0.000 |
| Linear | 4 | 12,028.8 | 12,028.8 | 3007.19 | 99.68 | 0.000 |
| N | 1 | 2.7 | 2.7 | 2.67 | 0.09 | 0.769 |
| Y | 1 | 4129.1 | 4129.1 | 4129.13 | 136.87 | 0.000 |
| Z | 1 | 7378 | 7378 | 7378.03 | 244.56 | 0.000 |
| H | 1 | 518.9 | 518.9 | 518.94 | 17.2 | 0.000 |
| Square | 3 | 1101.2 | 1101.2 | 367.08 | 12.17 | 0.000 |
| N*N | 1 | 48.9 | 102.1 | 102.12 | 3.38 | 0.081 |
| Z*Z | 1 | 373.7 | 447.1 | 447.06 | 14.82 | 0.001 |
| H*H | 1 | 678.6 | 678.6 | 678.6 | 22.49 | 0.000 |
| 2-way interaction | 4 | 1622.3 | 1622.3 | 405.58 | 13.44 | 0.000 |
| N*Z | 1 | 240.3 | 240.2 | 240.25 | 7.96 | 0.011 |
| N*H | 1 | 96 | 96 | 96.04 | 3.18 | 0.09 |
| Y*Z | 1 | 331.2 | 331.2 | 331.24 | 10.98 | 0.003 |
| Z*H | 1 | 954.8 | 954.8 | 954.81 | 31.65 | 0 |
| Error | 20 | 603.4 | 603.4 | 30.17 | | |
| Lack-of-fit | 15 | 521.7 | 521.7 | 34.78 | 2.13 | 0.207 |
| Pure error | 5 | 81.7 | 81.7 | 16.34 | | |
| Total | 31 | 15,355.7 | | | | |

| S | R-sq | R-sq (adj) | Press | R-sq (pred) |
|---|---|---|---|---|
| Model summary | | | | |
| 5.4926 | 96.07% | 93.91% | 2146.94 | 86.02% |
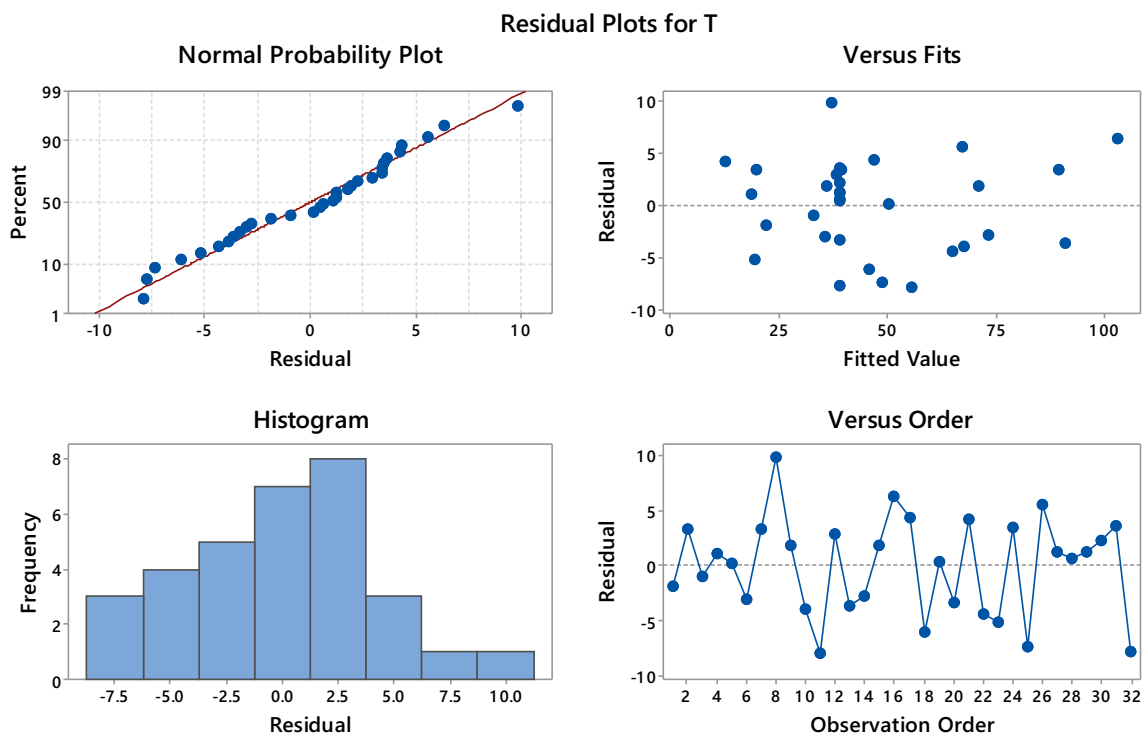


**Fig. 21** Residual plots for temperature rise

**Fig. 22** Main effects plot for temperature rise
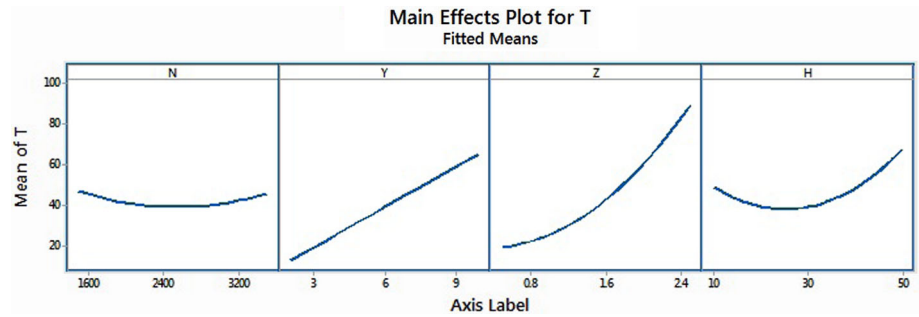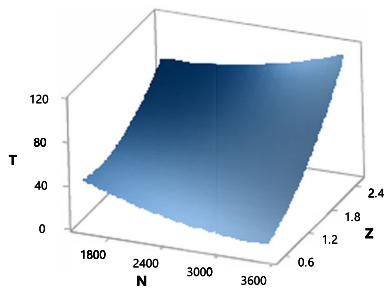


**Fig. 23** Effects of spindle speed and axial depth of cut on T
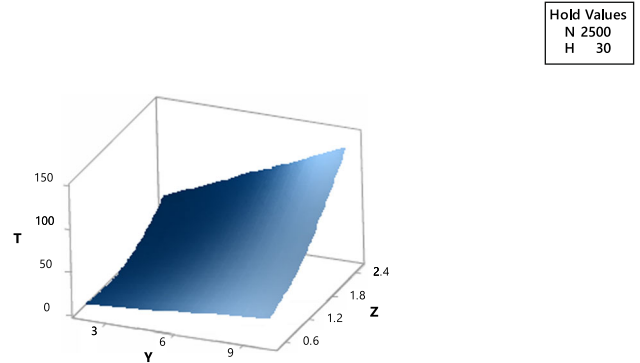


**Fig. 24** Effects of spindle speed and helix angle on T



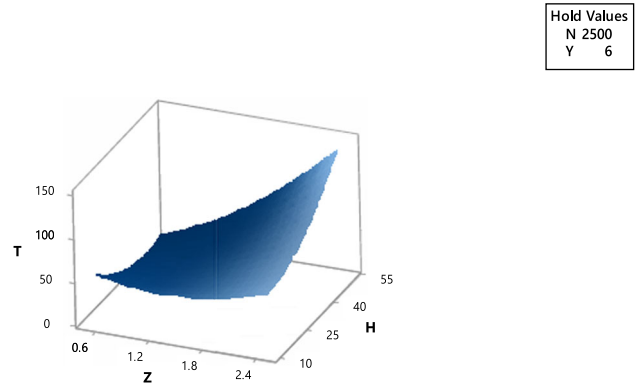**Fig. 25** Effects of radial and axial depth of cut on T
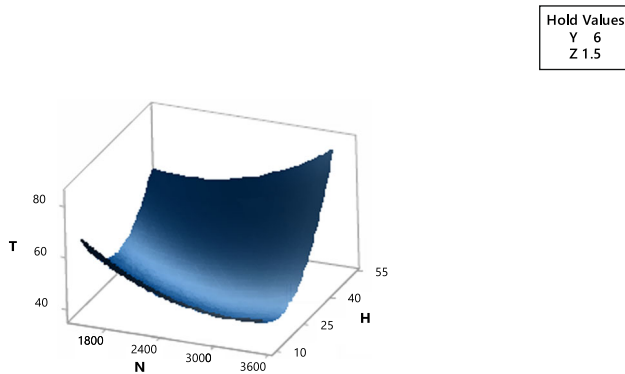


**Fig. 26** Effects of axial depth of cut and helix angle on T

temperature rise with the increase in helix angle up to 30° was observed, the trend was reversed for higher helix angle. This was like the observations of Sivasakthivel et al. [44]. The friction of tool-chip interface increases with increase in helix angle, resulting in to the obstruction to chip flow and the slowness of dispersal out of cutting heat, resulting in the increasing of temperature [57]. The lower depth of cut with moderate helix angle and spindle speed was found to help in reducing the temperature rise.

The surface plot of effects of spindle speed and axial depth of cut on temperature rise is shown in Fig. 23. The rise in the temperature was found to be smaller when the combination of the higher spindle speed and smaller depth of cut was used. At higher spindle speed and higher depth of cut the temperature rise was higher. The surface plot of the effects of spindle speed and helix angle on rise of the temperature (Fig. 24) also shows that the temperature rise reduces when the spindle speed increases. The moderate value of the helix angle and higher spindle speed combination resulted in to reduction in the temperature. The surface plot of the effects of radial and axial depth of cut on temperature rise (Fig. 25), shows that increase in the values of the depth of cut resulted

in to the increase in the value of rise in temperature. It can also be seen that the effect of axial depth of cut is stronger than the effect of radial depth of cut. The effect of the axial depth of cut on rise in temperature was found to be more with higher helix angle tool (Fig. 26). For higher helix angle the temperature rise was more significant particularly for larger axial depth of cut. It indicates that, the higher helix angle tool with smaller axial depth of cut can control the rise in temperature effectively.

### 4.3 Model generation for surface roughness

The surface roughness was measured after the completion of all the experiments. Second order quadratic model was developed using the response surface method. Analysis of variance was done to find out the effective parameters in the developed model and the non-effective parameters were removed by backward elimination method. Table 10 shows the ANOVA results for Ra along with the model summary. The second order model in uncoded units is as shown in Eq. (8).

$$
\begin{aligned}
\text{Ra} =\ & 3.752 - 0.000478N - 0.00418F \\
& - 0.1212Y - 2.857Z - 0.0312H + 0.01189Y*Y \\
& + 0.6087Z*Z + 0.000819H*H + 0.000353N*Z \\
& + 0.00415F*Z - 0.01633Z*H
\end{aligned}
\tag{8}
$$

This model has got the R-sq value of 91.28% which means the model explains that the experimental data well. Also, the R-sq value for the model was close to the adjusted coefficient of determination value of the model (R-sq (adj) = 86.48%) and value of R-sq (pred) was in reasonable agreement with the R-sq (adj). The F-value of model was 19.02, it means that model was significant. The F value for lack of fit was 3.11 and $p$ value was 0.108 indicates insignificant lack of fit. Figure 27 shows the residual plots for surface roughness in order to check the model adequacy, in the normal probability plot the residuals were following a straight line and in the versus fit plot the residuals were randomly scattered about the zero line. The histogram and residuals versus order graphs also indicates that fitted model values were closer to the experimental values. The main effects plot for the surface roughness (Fig. 28) shows that the spindle speed has little effect on the surface roughness value and Ra value increases with increase in speed and feed rate. The increase in spindle speed reduces tendency of formation of built-up edge but will also results in to more vibrations so surface get deteriorated at higher spindle speed [34]. The surface gets deteriorated with higher feed rate as the tool transverse the workpiece too fast at the higher feed rate [58]. The similar observations were also reported by Reddy et al. [59] and Singh et al. [60]. The

moderate values of depth of cut and helix angle were producing better surface. During the light finish cuts; built edge formation, feed marks and vibrations are less as a smaller amount of material is removed, which gives better finish. As helix angle increases the Ra value reduces as the increase in helix angle reduces the shock load and vibrations and thus results in to better surface [39].

The effects of axial depth of cut and spindle speed on Ra are shown in Fig. 29. The Ra value was found to be lower for smaller depth of cut and higher spindle speed. The surface deterioration was more severe when the large axial depth of cut was used along with higher spindle speed. The Fig. 30 shows effects of axial depth of cut and feed rate on Ra, here also, lower Ra value was noticed for smaller depth of cut and higher spindle speed, the increase in the axial depth of cut was resulting in deterioration of the surface [60].

Figure 31 shows the effects of axial depth of cut and helix angle on Ra. The Ra value was found to be lower when depth of cut was around 1.5 mm and helix angle of 30°. The roughness was found to be more when large depth of cut was used.

## 5 Multi-objective optimization

In the current work, multi-objective optimization was performed for minimization of optimization of total energy consumed, surface roughness, rise of workpiece surface temperature and for maximization of energy efficiency and power factor. Individual response functions found out after backward elimination method (Eqs. 4, 5, 6, 7, 8) were used. The desirability analysis was used for finding out the optimum values of the process parameters.

### 5.1 Response optimization with desirability approach

The multi objective problems are normally complex to solve, to simplify it, the desirability function analysis (DFA) method was proposed by Derringer et al. [61] and currently, this method is extensively adopted by the industries for the multi-objective optimisations[62, 63]. It is an interesting method to find out the apt settings of the input parameters in order to get the optimum results and particularly useful for multi objective problems. [32, 64]. Initially each response variable is converted into a dimensionless scale-free desirability value ($di$) (using Eqs. 8 and 9) in the scale of zero to one; where zero means an entirely undesirable response and one means an entirely desired response [64]. Equation (9) is used for larger the better characteristic and Eq. (10) for smaller is better characteristic [65].

$$
di = \left( \frac{f_i - f_{imin}}{f_{imax} - f_{imin}} \right)^w
\tag{9}
$$

**Table 10** ANOVA results for Ra

| Source | DF | Seq SS | Adj SS | Adj MS | F-value | P-value |
|---|---|---|---|---|---|---|
| Model | 11 | 2.63871 | 2.63871 | 0.23988 | 19.02 | 0 |
| Linear | 5 | 1.36586 | 1.36586 | 0.27317 | 21.66 | 0 |
| N | 1 | 0.01612 | 0.01612 | 0.01612 | 1.28 | 0.272 |
| F | 1 | 0.24807 | 0.24807 | 0.24807 | 19.67 | 0 |
| Y | 1 | 0.04403 | 0.04403 | 0.04403 | 3.49 | 0.076 |
| Z | 1 | 0.95441 | 0.95441 | 0.95441 | 75.68 | 0 |
| H | 1 | 0.10323 | 0.10323 | 0.10323 | 8.19 | 0.01 |
| Square | 3 | 0.86948 | 0.86948 | 0.28983 | 22.98 | 0 |
| Y*Y | 1 | 0.03061 | 0.06718 | 0.06718 | 5.33 | 0.032 |
| Z*Z | 1 | 0.63944 | 0.68808 | 0.68808 | 54.56 | 0 |
| H*H | 1 | 0.19942 | 0.19942 | 0.19942 | 15.81 | 0.001 |
| 2-way interaction | 3 | 0.40337 | 0.40337 | 0.13446 | 10.66 | 0 |
| N*Z | 1 | 0.12496 | 0.12496 | 0.12496 | 9.91 | 0.005 |
| F*Z | 1 | 0.17181 | 0.17181 | 0.17181 | 13.62 | 0.001 |
| Z*H | 1 | 0.1066 | 0.1066 | 0.1066 | 8.45 | 0.009 |
| Error | 20 | 0.25222 | 0.25222 | 0.01261 | | |
| Lack-of-fit | 15 | 0.2278 | 0.2278 | 0.01519 | 3.11 | 0.108 |
| Pure error | 5 | 0.02442 | 0.02442 | 0.00488 | | |
| Total | 31 | 2.89093 | | | | |

| S | R-sq | R-sq (adj) | Press | R-sq (pred) | |
|---|---|---|---|---|---|
| **Model summary** | | | | | |
| 0.112299 | 91.28% | 86.48% | 0.84104 | 70.91% | |

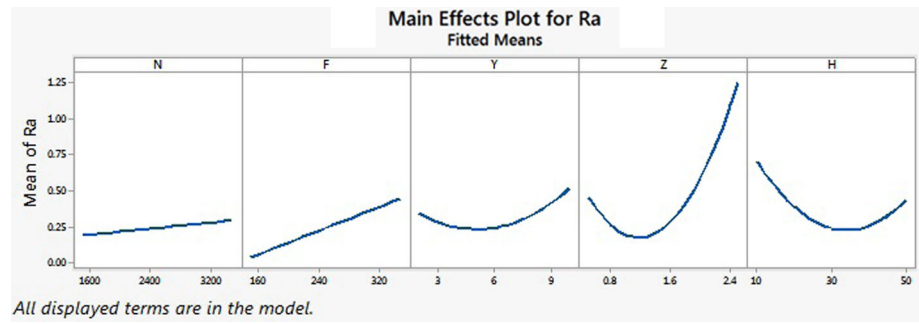### Residual Plots for Ra
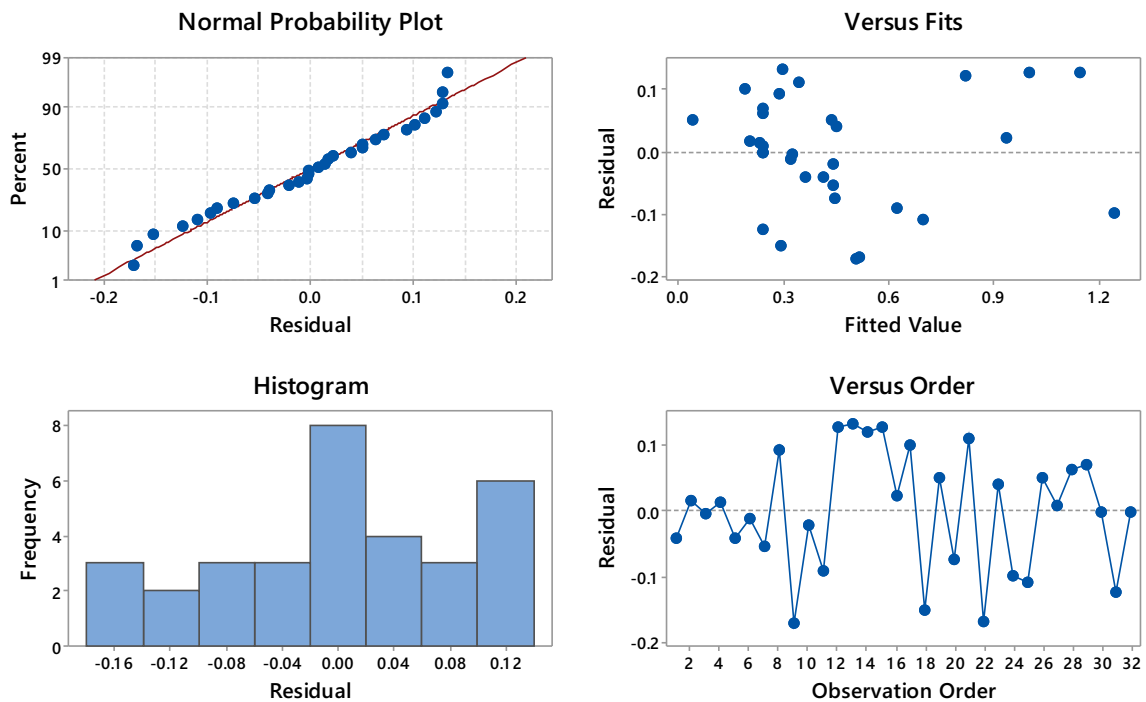


**Fig. 27** Residual plots for surface roughness

**Fig. 28** Main effects plot for Ra
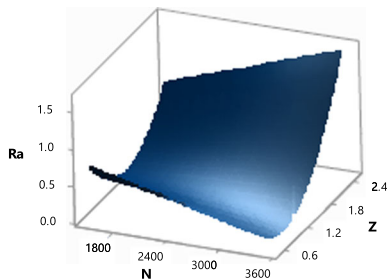


**Surface Plot of Ra vs Z, N**



**Fig. 29** Effects of axial depth of cut and spindle speed on Ra
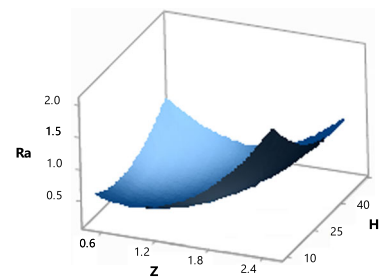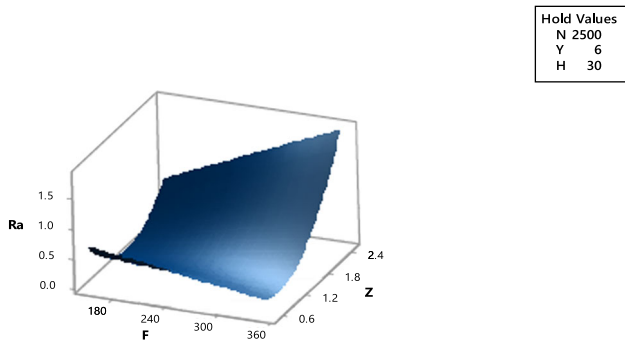
**Surface Plot of Ra vs Z, F**



**Fig. 30** Effects of axial depth of cut and feed rate on Ra

The individual desirability, $d_i = 1$ when $f_i \geq f_{i\,max}$; $d_i = 0$, when $f_i \leq f_{i\,min}$.

$$di = \left( \frac{f_{imax} - f_i}{f_{imax} - f_{imin}} \right)^w \qquad (10)$$

The individual desirability, $d_i = 0$ when $f_i \geq f_{i\,max}$; $d_i = 1$, when $f_i \leq f_{i\,min}$.

Here, '$i$' designates the response and '$f$' designates the value of response, $f_{i\,min}$ indicates the minimum value of the response, $f_{imax}$ indicates the maximum value of the response and '$w$' is a weight used to determine scale of desirability

**Surface Plot of Ra vs H, Z**



**Fig. 31** Effects of Axial depth of cut and helix angle on Ra

[15]. The overall desirability (D) is determined with the help of geometric mean as shown in Eq. (11) as,

$$D = \left( \prod_{i=1}^{n} d_i^{w_i} \right)^{\frac{1}{\sum w_i}} \qquad (11)$$

Here $w_i$ is weight of individual response which changes between 1 to 5. The higher value of the overall desirability means best response function of the problem [15, 18].

The multi objective optimization was carried out for three different groups of response variables considering the different importance of energy consumption, cutting temperatures and surface roughness, under different manufacturing circumstances.

Group I: Simultaneous minimization of TECM and Ra; along with the maximization of EE and PF;
Group II: Minimization of the workpiece surface temperature and surface roughness were the targets;
Group III: All the responses were considered for the multi objective optimization.

**Table 11** Optimization criteria and desirability for Group I

| Name | Goal | Lower limit | Upper limit | Lower weight | Upper weight | Importance | Desirability |
|------|------|-------------|-------------|--------------|--------------|------------|--------------|
| N | Is in range | 1500 | 3500 | 1 | 1 | 3 | 1 |
| F | Is in range | 150 | 350 | 1 | 1 | 3 | 1 |
| Y | Is in range | 2 | 10 | 1 | 1 | 3 | 1 |
| Z | Is in range | 0.5 | 2.5 | 1 | 1 | 3 | 1 |
| H | Is in range | 10 | 50 | 1 | 1 | 3 | 1 |
| TECM | Minimize | 20,202 | 41,607 | 1 | 1 | 5 | 0.846 |
| EE | Maximize | 4.480287 | 37.0595 | 1 | 1 | 5 | 0.908 |
| Ra | Minimize | 0.088 | 1.273 | 1 | 1 | 3 | 0.449 |
| PF | Minimize | 0.768 | 0.865 | 1 | 1 | 5 | 0.997 |
| Composite desirability | – | – | – | – | – | – | 0.813 |
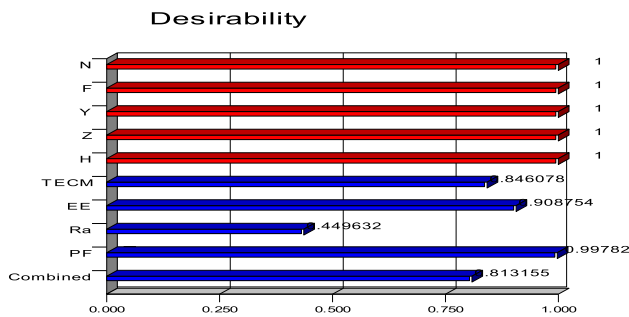


**Fig. 32** Bar chart for desirability for Group I

## 5.2 Multi objective optimization for TECM, PF, EE, and Ra (Group I)

The lower limit, upper limit, and the weight of all the process parameters for this multi objective optimization are shown in Table 11. Here equal importance was given to TECM, PF and PF because these parameters were directly affecting sustainability of machining operation and slightly less importance was given to Ra as the operation was a roughing operation [15, 52].

The optimum values of parameters were found as: spindle speed: 1500 rpm, feed rate: 350 mm/min, axial depth of cut: 1.27 mm, radial depth of cut: 7.15 mm and helix angle: 10° for better machining performance in terms of minimum TECM, minimum Ra, maximum EE, and maximum PF. The response parameters obtained with these input factors were, TECM = 23,496.7 J, EE = 34.08%, PF = 0.865 and Ra = 0.74 µm.

Figure 32 shows the bar graph for each factor and each response individually, the bottom histogram bar is the overall desirability of all the responses. The contour plots for overall desirability is as shown in Fig. 33. The composite desirability value of 0.813 was located on the top left-hand side region of the plot and Fig. 34 shows the desirability ramp for numerical

optimisation indicating the desirability for each factor and each response, as well as the combined desirability.

## 5.3 Multi objective optimization for T and Ra (Group II)

The lower and upper limits along with the weight of all the process parameters for this multi objective optimization are shown in Table 12. Here more importance was given to T and slightly less importance was given to Ra as the operation was a roughing operation. The optimum values of parameters are found as: Spindle speed: 3257.46 rpm, feed rate: 291 mm/min, axial depth of cut: 0.71 mm, radial depth of cut: 4.50 mm and helix angle: 30° for better machining performance in terms of minimization of rise in the workpiece surface temperature and Ra.

The response parameters obtained with these input factors were, T = 10.91 °C and Ra = 0.077 µm.

Figure 35 shows the bar graph for each factor and each response individually, the bottom histogram bar is the overall desirability of all the responses. The contour plots for overall desirability is as shown in Fig. 36. The composite desirability value of 1.00 was located on the top right-hand side region of the plot. Figure 37, shows the desirability ramp for each factor and response, along with the combined desirability.

## 5.4 Multi objective optimization for all responses (Group III)

The lower limit, upper limit, and the weight of all the process parameters for this multi objective optimization are shown in Table 13. Here equal importance was given to TECM, EE, PF and T because these parameters were affecting sustainability of machining operation and slightly less importance was given to Ra as the operation was a roughing operation.

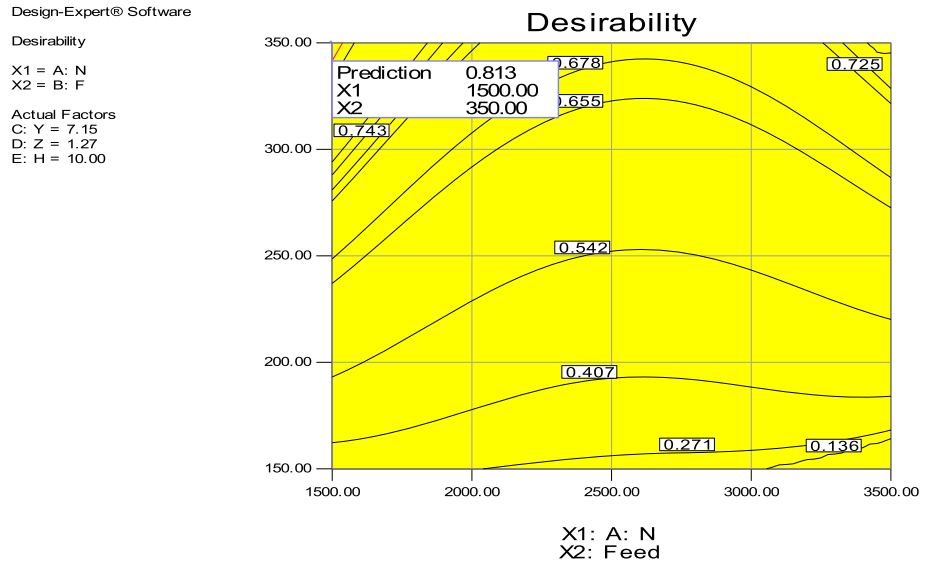**Fig. 33** Contour plots of overall desirability for Group I
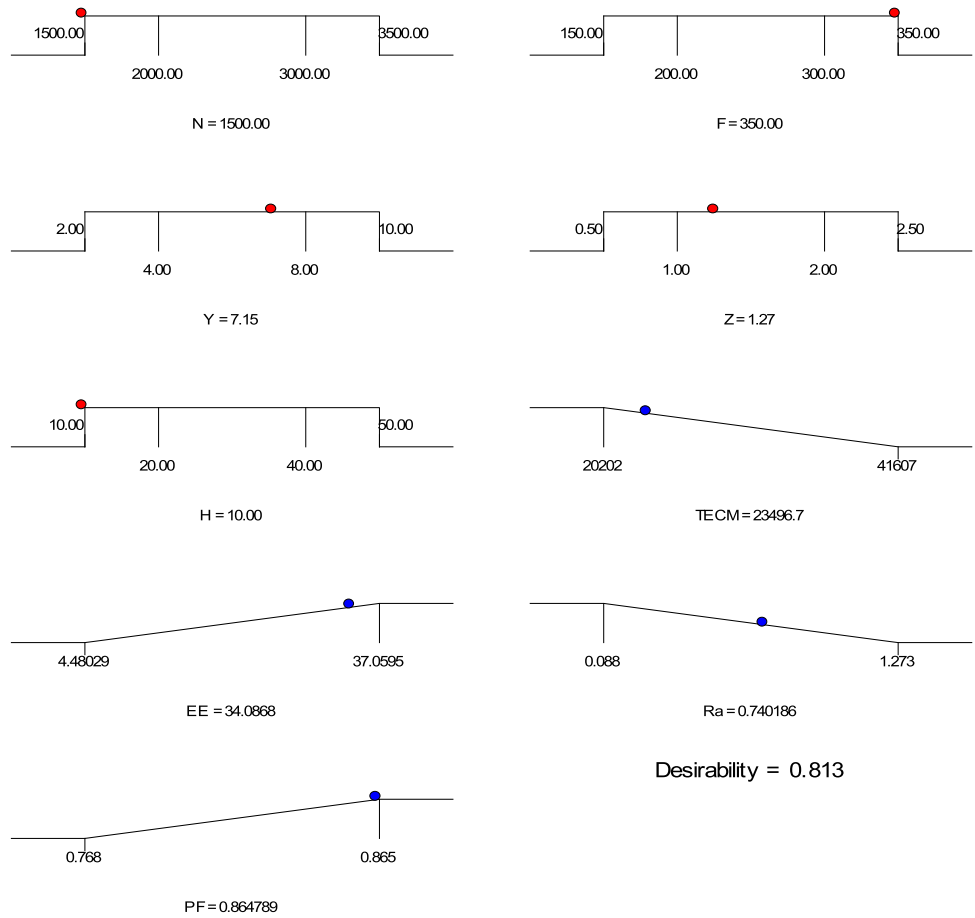


**Fig. 34** Desirability ramp for TECM, PF, EE, and Ra

**Table 12** Optimization criteria and desirability for Group II

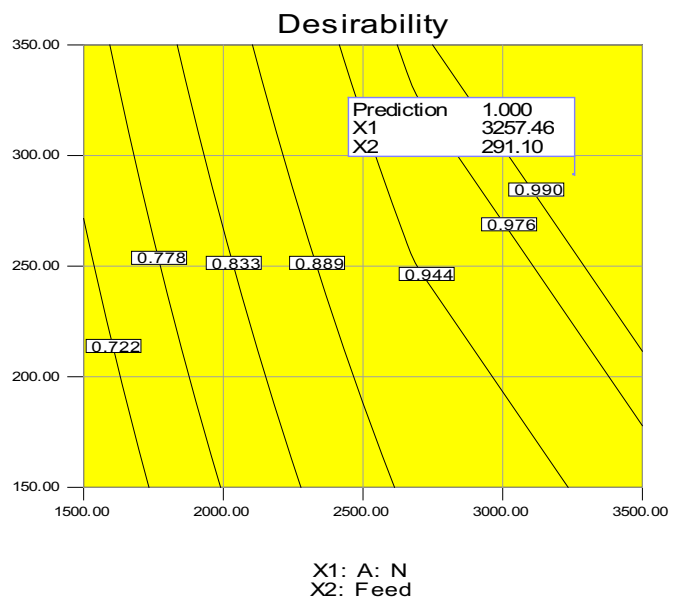| Name | Goal | Lower limit | Upper limit | Lower weight | Upper weight | Importance | Desirability |
|------|------|-------------|-------------|--------------|--------------|------------|--------------|
| N | Is in range | 1500 | 3500 | 1 | 1 | 3 | 1 |
| F | Is in range | 150 | 350 | 1 | 1 | 3 | 1 |
| Y | Is in range | 2 | 10 | 1 | 1 | 3 | 1 |
| Z | Is in range | 0.5 | 2.5 | 1 | 1 | 3 | 1 |
| H | Is in range | 10 | 50 | 1 | 1 | 3 | 1 |
| T | Minimize | 14.2 | 109.4 | 1 | 1 | 5 | 1 |
| Ra | Minimize | 0.088 | 1.273 | 1 | 1 | 3 | 1 |
| Composite desirability | | | | | | | 1 |
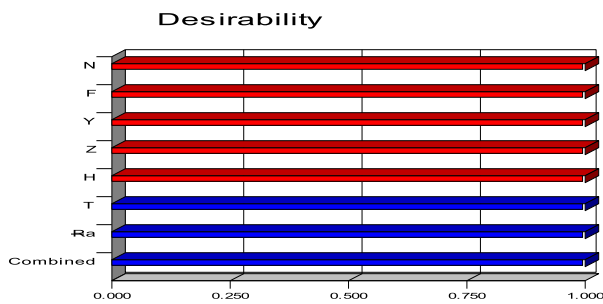


**Fig. 35** Bar chart for desirability for Group II

The optimum values of parameters are found as: spindle speed: 3500 rpm, feed rate: 350 mm/min, axial depth of cut: 0.74 mm, radial depth of cut: 2.86 mm and helix angle: 50° for better machining performance in terms of minimum T, minimum TECM, minimum Ra, maximum EE, and maximum PF. The response parameters obtained with these input factors were, T = 21.32, TECM = 25,601.9 J, EE = 26.67%, PF = 0.857 and Ra = 0.454 μm.

Figure 38 shows the bar graph for each factor and each response individually, the bottom histogram bar is the composite desirability of all the responses. The contour plots for overall desirability is as shown in Fig. 39. The composite desirability value of 0.794 was located on the top right-hand side region of the plot. The desirability ramp for all the factors and responses, in addition to the composite desirability is shown in Fig. 40.

## 5.5 Confirmation experiments

In order to verify the adequacy of the model developed and for the confirmation of the optimized results, milling operations were carried out on EN 8 at the optimized settings
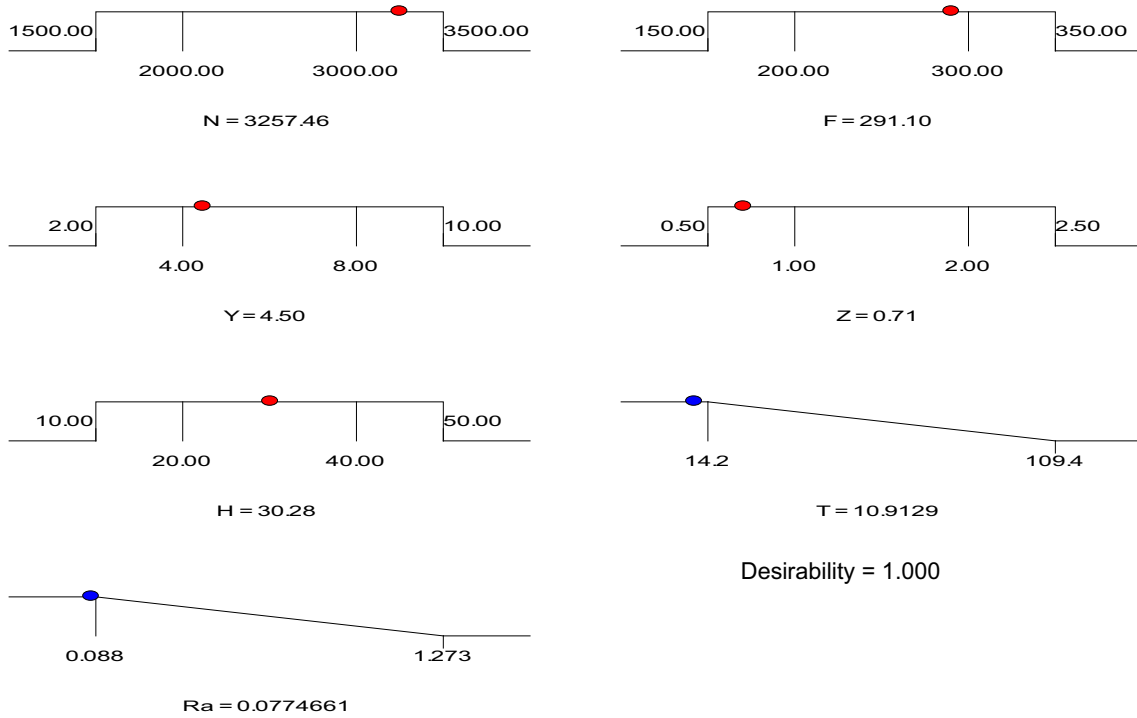
**Fig. 36** Contour plots of overall desirability for Group II

**Fig. 37** Desirability ramp for T and Ra

**Table 13** Optimization criteria and desirability for all responses

| Name | Goal | Lower limit | Upper limit | Lower weight | Upper weight | Importance | Desirability |
|---|---|---|---|---|---|---|---|
| N | Is in range | 1500 | 3500 | 1 | 1 | 3 | 1 |
| F | Is in range | 150 | 350 | 1 | 1 | 3 | 1 |
| Y | Is in range | 2 | 10 | 1 | 1 | 3 | 1 |
| Z | Is in range | 0.5 | 2.5 | 1 | 1 | 3 | 1 |
| H | Is in range | 10 | 50 | 1 | 1 | 3 | 1 |
| T | Minimize | 14.2 | 109.4 | 1 | 1 | 5 | 0.925 |
| TECM | Minimize | 20,202 | 41,607 | 1 | 1 | 5 | 0.747 |
| EE | Maximize | 4.48029 | 37.0595 | 1 | 1 | 5 | 0.681 |
| Ra | Minimize | 0.088 | 1.273 | 1 | 1 | 3 | 0.690 |
| PF | Maximize | 0.768 | 0.865 | 1 | 1 | 5 | 0.918 |
| Composite desirability | | | | | | | 0.794 |
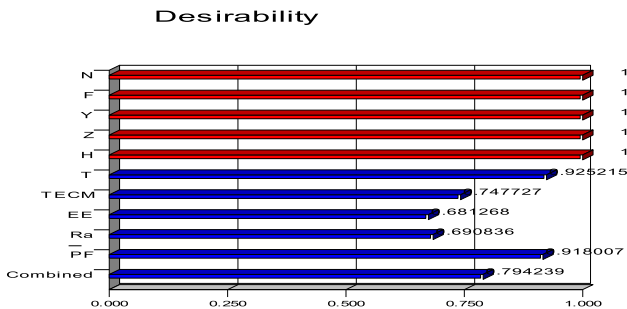


**Fig. 38** Bar chart for desirability for Group III

for all the scenarios considered and average values of all the responses for of two actual experiments were calculated. The comparison of test results and the predicted values obtained by using the regression equations was made and presented in Table 14. The predicted values and the experimental values are found to be very near to each other. For dependable statistical analyses, percentage error between the predicted values and the experimental values must be less than 20% [66]. It was found within the acceptable limits.

**Fig. 39** Contour plots for overall desirability for Group III



Design-Expert® Software

Desirability

X1 = A: N
X2 = B: F
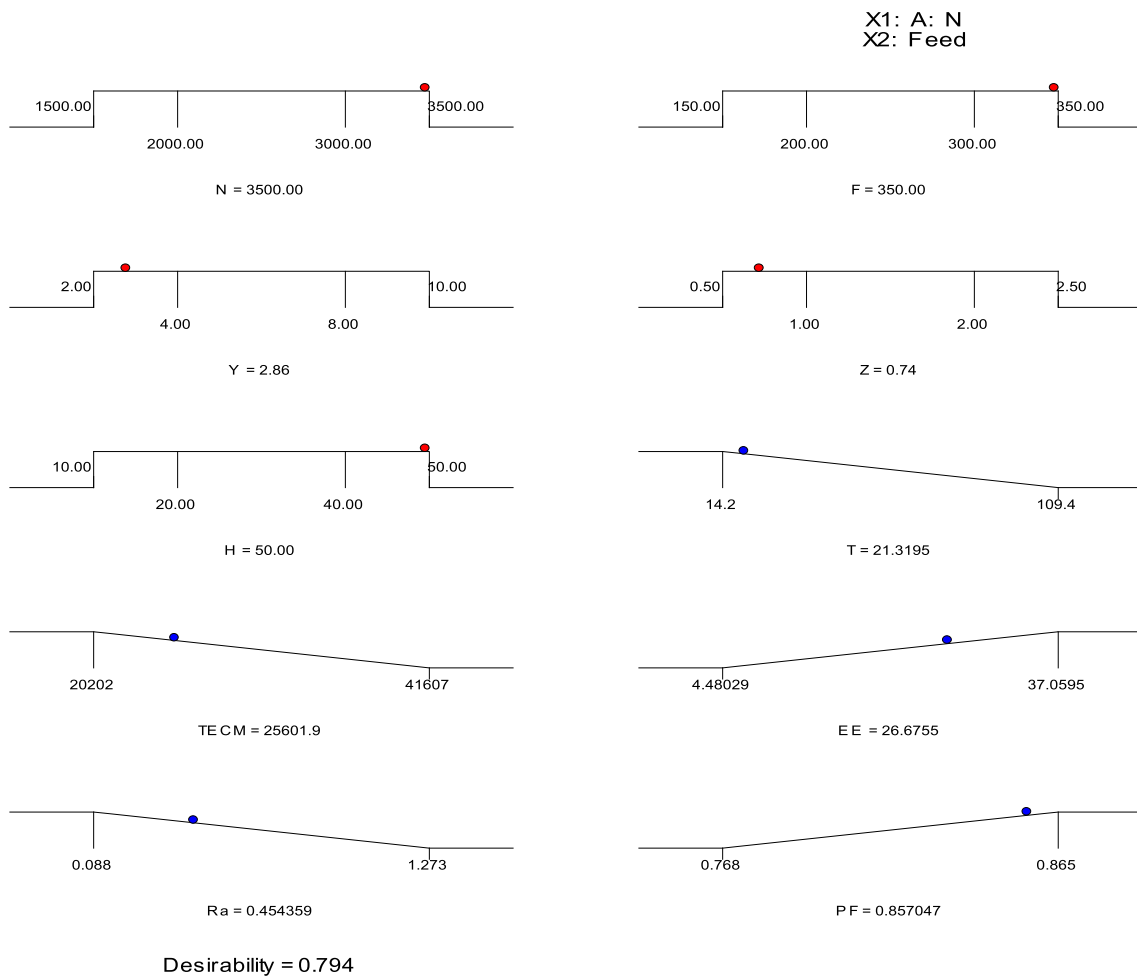
Actual Factors
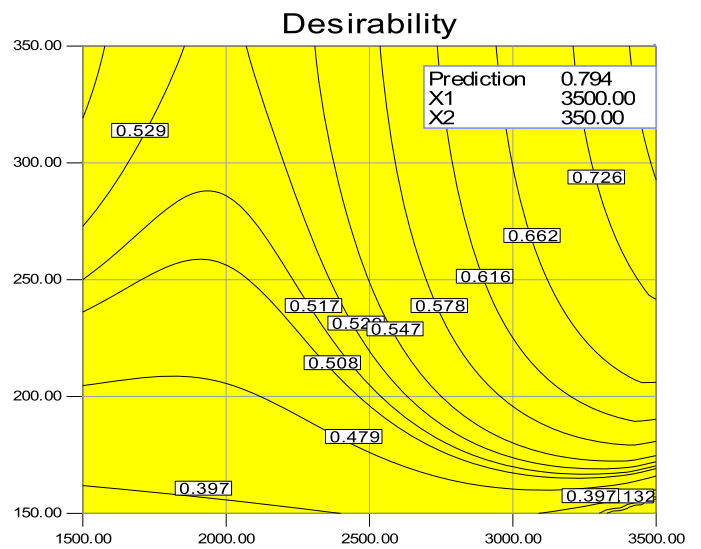C: Y = 2.86
D: Z = 0.74
E: H = 50.00



**Fig. 40** Desirability ramp for all responses

**Table 14** Validation results with optimized parameters for EN 8

| Response parameter | Predicted by RSM | Experimental average value | % error |
|---|---|---|---|
| a. For TECM, EE, PF and Ra | | | |
| TECM | 23,496.7 | 22,000 | − 6.80 |
| EE | 34.087 | 32.58 | − 4.63 |
| PF | 0.865 | 0.859 | − 0.70 |
| Ra | 0.74 | 0.7755 | 4.58 |
| b. For T and Ra | | | |
| T | 10.91 | 12.05 | 9.46 |
| Ra | 0.077 | 0.086 | 10.47 |
| c. For all responses | | | |
| T | 21.31 | 19.7 | − 8.17 |
| TECM | 25,601 | 23,232 | − 10.20 |
| EE | 26.675 | 24.58 | − 8.52 |
| PF | 0.857 | 0.827 | − 3.63 |
| Ra | 0.454 | 0.5 | 9.20 |

# 6 Conclusions

In the present study, a successful application of RSM for analysing the response parameters like total energy consumption, energy efficiency, power factor, workpiece temperature rise and surface roughness in milling process is demonstrated. Five levels of each input process parameters viz, spindle speed, feed rate, radial depth of cut, axial depth of cut and helix angle were used for the experimentation. Predictive models were formulated and effects of these process parameters on the responses were studied and presented in graphical form. The optimization of process parameters was carried out by desirability analysis. The multi objective optimization was carried out for three different situations as the weightage of the response parameters is altering under diverse manufacturing conditions. This work evaluates the trade-offs between energy, heat generation and cutting quality.

Based on above work, following conclusions are drawn:

1. During the experimentation on EN 8, it was established that RSM is a powerful tool in order to develop predictive mathematical models to predict responses correctly and to analyse the effects of the process parameters by plotting response surfaces.
2. The predictability of the multiple regression approach was found to be more than 90% showing capability of the models to explain the experimental data. All the models were having $p$ values less than 0.05 and lack of fit $p$ values more than 0.05, indicates that the models were significant within 95% confidence interval.
3. The feed rate was most significant parameter for total energy consumption, followed by axial and radial depth of cut. The energy consumption was reducing with increase in feed rate; due to reduction in total cycle time. The lesser values of depth of cuts and spindle speeds were also contributing in reducing energy consumed. The role of helix angle was found to be insignificant with respect to the energy consumption.
4. The most significant factors affecting energy efficiency and power factor in descending order were axial depth of cut, radial depth of cut and helix angle. Better efficiency was observed for larger values of depth of cuts, helix angle and feed rate. Power factors was found to be increasing when the motor was drawing more power.
5. The axial depth of cut was highly significant for the temperature rise followed by radial depth of cut and helix angle. Higher the depth of cut result; more is the contact area between the tool and workpiece; which results in more temperatures. Spindle speed and feed rate were not having much effect on temperature rise.
6. The surface roughness was mainly getting affected by axial depth of cut, followed by feed rate and helix angle. Better surface finish was obtained at smaller spindle speed and feed rate along with medium values of depth of cut and helix angle.
7. The values of the composite desirability achieved in all the three types of optimization situations were on the higher side (0.813, 1 and 0.794). This highlights capability of the desirability approach to achieve the desired goals of minimization and maximization. During the first situation of the optimization the individual desirability of surface roughness was less (d = 0.449), which suggests that the desired reduction was not achieved for surface roughness under the given conditions.
8. The results of the optimization were confirmed by conducting the experiments the optimized settings. The maximum percentage error between experimental and RSM predicted results was around 10%, which is within acceptable limits.
9. This study can be helpful for machine operators improving the sustainability by reducing the energy consumption and cutting temperatures and improving the power factor and energy efficiency without compromising on surface roughness, in the machining of medium carbon steel.
10. In future, researchers may consider the other geometrical features of the end mill like rake angle, dish angle etc. for this medium carbon steel EN-8, the use of coated tools may also be considered. These results can also be analysed using other evolutionary optimization

techniques such as genetic algorithm, teaching learning-based algorithm etc. The works can be carried out on advanced and difficult to machine materials like titanium alloys, nickel alloys and composites materials.

# References

1. Moradnazhad, M., Unver, H.O.: Energy efficiency of machining operations: a review Energy efficiency of machining operations: a review. Proc. IMechE Part B J. Eng. Manuf. **231**, 1871–1889 (2016). https://doi.org/10.1177/0954405415619345

2. Hayajneh, M.T., Tahat, M.S., Bluhm, J.: A study of the effects of machining parameters on the surface roughness in the end-milling process. Jordan J. Mech. Indust. Eng. **1**(1), 1–5 (2007)

3. Newman, S.T., Nassehi, A., Dhokia, V.: Energy efficient process planning for CNC machining. CIRP J. Manuf. Sci. Technol. **5**(2), 127–136 (2012). https://doi.org/10.1016/j.cirpj.2012.03.007

4. Bilga, P.S., Singh, S., Kumar, R.: Optimization of energy consumption response parameters for turning operation using Taguchi method. J. Clean. Prod. **137**, 1406–1417 (2016). https://doi.org/10.1016/j.jclepro.2016.07.220

5. Kuram, E., Ozcelik, B., Bayramoglu, M., Demirbas, E., Tolga, B.: Optimization of cutting fluids and cutting parameters during end milling by using D-optimal design of experiments. J. Clean. Prod. **42**, 159–166 (2013). https://doi.org/10.1016/j.jclepro.2012.11.003

6. Campatelli, G., Lorenzini, L., Scippa, A.: Optimization of process parameters using a Response Surface Method for minimizing power consumption in the milling of carbon steel. J. Clean. Prod. **66**, 309–316 (2014). https://doi.org/10.1016/j.jclepro.2013.10.025

7. Yan, J., Li, L.: Multi-objective optimization of milling parameters – the trade-offs between energy, production rate and cutting quality. J. Clean. Prod. **52**, 462–471 (2013). https://doi.org/10.1016/j.jclepro.2013.02.030

8. Zhang, C., Li, W., Jiang, P., Gu, P.: Experimental investigation and multi-objective optimization approach for low-carbon milling operation of aluminum. Proc. IMechE Part C J. Mech. Eng. Sci. (2016). https://doi.org/10.1177/0954406216640574

9. Öztürk, B., Kara, F.: Calculation and estimation of surface roughness and energy consumption in milling of 6061 alloy. Adv. Mater. Sci. Eng. **2020**, 1–12 (2020). https://doi.org/10.1155/2020/5687951

10. Kadirgama, K., Abou-El-Hossein, K.A.: Power prediction model for milling 618 stainless steel using response surface methodology. Am. J. Appl. Sci. **2**(7), 1182–1187 (2005)

11. Kadirgama, K., Abou-El-Hossein, K.A.: Torque, power and cutting force prediction model by using response surface method and factorial design. Edit. Adv. Board e **18**(1), 20–44 (2005)

12. Bağcı, E., Aykut, Ş: The effects of tool position, coating and cutting parameters on forces, power, MRR and wear in face milling of stellite 6. Arabian J. Sci. Eng. **39**(11), 8135–8146 (2014). https://doi.org/10.1007/s13369-014-1354-6

13. Ahmed, S.U., Arora, R.: Quality characteristics optimization in CNC end milling of A36 K02600 using Taguchi's approach coupled with artificial neural network and genetic algorithm. Int. J. Syst. Assur. Eng. Manag. **10**(4), 676–695 (2019). https://doi.org/10.1007/s13198-019-00796-8

14. Noor, R.M., Ramli, M.I., Zubair, A.F., Hemdi, A.R., Kataraki, P.: Optimization of cutting parameters to improve power consumption and material removal rate in high efficiency milling. J. Mines Metals Fuels **69**(12A), 163 (2022). https://doi.org/10.18311/jmmf/2021/30149

15. Sahu, N.K., Andhare, A.B.: Modelling and multiobjective optimization for productivity improvement in high speed milling of Ti–6Al–4V using RSM and GA. J. Brazil. Soc. Mech. Sci. Eng. **39**(12), 5069–5085 (2017). https://doi.org/10.1007/s40430-017-0804-y

16. Malghan, R.L., Rao, K.M.C., Shettigar, A.K., Rao, S.S., D'Souza, R.J.: Application of particle swarm optimization and response surface methodology for machining parameters optimization of aluminium matrix composites in milling operation. J. Brazil. Soc. Mech. Sci. Eng. **39**(9), 3541–3553 (2016). https://doi.org/10.1007/s40430-016-0675-7

17. Helu, M., Rühl, J., Dornfeld, D., Werner, P., Lanza, G.: Evaluating trade-offs between sustainability, performance, and cost of green machining technologies. In 18th CIRP International Conference on Life Cycle Engineering, pp. 195–200. (2011). https://doi.org/10.1007/978-3-642-19692-8

18. Bhushan, R.K.: Optimization of cutting parameters for minimizing power consumption and maximizing tool life during machining of Al alloy SiC particle composites. J. Clean. Prod. **39**, 242–254 (2013). https://doi.org/10.1016/j.jclepro.2012.08.008

19. Aggarwal, A., Singh, H., Kumar, P., Singh, M.: Optimizing power consumption for CNC turned parts using response surface methodology and Taguchi's technique—A comparative analysis. J. Mater. Process. Technol. **200**(1–3), 373–384 (2008). https://doi.org/10.1016/j.jmatprotec.2007.09.041

20. Fata, A.: Temperature measurement during machining depending on cutting conditions. G. J. P A Sci. Tech. **1**(2), 16–21 (2011)

21. Bacci, M., Wallbank, J.: Cutting temperature: prediction and measurement methods—a review. J. Mater. Process. Tech. **88**, 195–202 (1999)

22. Bhirud, N.L., Gawande, R.R.: Measurement and prediction of cutting temperatures during dry milling: review and discussions. J. Brazil. Soc. Mech. Sci. Eng. **39**(12), 5135–5158 (2017). https://doi.org/10.1007/s40430-017-0869-7

23. Tamilarasan, A., Marimuthu, K., Renugambal, A.: Investigations and optimization for hard milling process parameters using hybrid method of RSM and NSGA-II. Rev. Téc. Ing. Univ. Zulia. **39**(2012), 41–54 (2016)

24. Tamilarasan, A., Marimuthu, K.: Multi-response optimization of hard milling process: RSM coupled with grey relational analysis. Int. J. Eng. Technol. **5**(6), 4901–4913 (2014)

25. Tamilarasan, A., Marimuthu, K.: Multi-response optimisation of hard milling process parameters based on integrated Box-Behnken design with desirability function approach. Int. J. Mach. Mach. Mater **15**(3/4), 300 (2014). https://doi.org/10.1504/IJMMM.2014.060555

26. M. H. F. Al Hazza, E. Y. T. Adesta, M. Y. Superianto, M. Riza, Cutting temperature and surface roughness optimization in CNC end milling using multi objective genetic algorithm. In Proceedings - 2012 International Conference on Advanced Computer Science Applications and Technologies, ACSAT 2012, pp. 275–278. (2013). https://doi.org/10.1109/ACSAT.2012.39.

27. Le Coz, G., Marinescu, M., Devillez, A., Dudzinski, D., Velnom, L.: Measuring temperature of rotating cutting tools: application to MQL drilling and dry milling of aerospace alloys. Appl. Thermal Eng. **36**, 434–441 (2012). https://doi.org/10.1016/j.applthermaleng.2011.10.060

28. Li, A., Zhao, J., Pei, Z., Zhu, N.: Simulation-based solid carbide end mill design and geometry optimization. Int. J. Adv. Manuf. Technol. **71**(9–12), 1889–1900 (2014). https://doi.org/10.1007/s00170-014-5638-5

29. Dinc, C., Lazoglu, I., Serpenguzel, A.: Analysis of thermal fields in orthogonal machining with infrared imaging. J. Mater. Technol. **198**(1–3), 147–154 (2008). https://doi.org/10.1016/j.jmatprotec.2007.07.002

30. Vikas, V., Shyamraj, R., Varughese, A.K.: Experimental study of the influence of tool geometry by optimizing helix angle in the peripheral milling operation using Taguchi based grey relational analysis. Int. J. Adv. Eng. Manag. Sci. **2**(8), 239594 (2016)

31. Izamshah, R., Yuhazri, M. Y., Hadzley, M., Amran, M. A.: Effects of end mill helix angle on accuracy for machining thin-rib aerospace component. vol. 315, pp. 773–777. (2013) https://doi.org/10.4028/www.scientific.net/AMM.315.773.

32. Sivasakthivel, P.S., Murugan, V.V., Sudhakaran, R.: Prediction of tool wear from machining parameters by response surface methodology in end milling. Int. J. Eng. Sci. Technol. **2**(6), 1780–1789 (2010)

33. Sivasakthivel, P.S., Velmurugan, V., Sudhakaran, R.: Prediction of vibration amplitude from machining parameters by response surface methodology in end milling. Int. J. Adv. Manuf. Technol. **53**, 453–461 (2011)

34. Sivasakthivel, P.S., Vel Murugan, V., Sudhakaran, R.: Experimental evaluation of surface roughness for end milling of Al 6063: response surface and neural network model. Int. J. Manuf. Res. **7**(1), 9–25 (2012)

35. Sivasakthivel, P.S., Vel Murugan, V., Sudhakaran, R.: Cutting force prediction depending on process parameters by response surface methodology in milling. Int. J. Mach. Mach. Mater. **11**(2), 137–153 (2012)

36. Hricova, J., Kovac, M., Sugar, P.: Experimental investigation of high speed milling of aluminium alloy. Tehnički Vjesnik **21**(4), 773–777 (2014)

37. Tsao, C.C.: Grey-Taguchi method to optimize the milling parameters of aluminum alloy. Int. J. Adv. Manuf. Technol. **40**(1–2), 41–48 (2009). https://doi.org/10.1007/s00170-007-1314-3

38. Kalidass, S., Palanisamy, P., Muthukumaran, V.: Prediction and optimisation of tool wear for end milling operation using artificial neural networks and simulated annealing algorithm. Int. J. Mach. Mach. Mater. **14**(2), 142 (2013). https://doi.org/10.1504/IJMMM.2013.055734

39. Kalidass, S., Palanisamy, P.: Prediction of surface roughness for AISI 304 steel with solid carbide tools in end milling process using regression and ANN models. Arab. J. Sci. Eng. **39**(11), 8065–8075 (2014). https://doi.org/10.1007/s13369-014-1346-6

40. Sivaraos, K.R., Milkey, A.R., Samsudin, A.K.: Comparison between Taguchi method and response surface. Jordan J. Mech. Ind. Eng. **8**(1), 35–42 (2014)

41. Kilickap, E., Huseyinoglu, M., Yardimeden, A.: Optimization of drilling parameters on surface roughness in drilling of AISI 1045 using response surface methodology and genetic algorithm. Int. J. Adv. Manuf. Technol. **52**(1–4), 79–88 (2011). https://doi.org/10.1007/s00170-010-2710-7

42. Santhanakrishnan, M., Sivasakthivel, P.S., Sudhakaran, R.: Modeling of geometrical and machining parameters on temperature rise while machining Al 6351 using response surface methodology and genetic algorithm. J. Brazil. Soc. Mech. Sci. Eng. **39**(2), 487–496 (2015). https://doi.org/10.1007/s40430-015-0378-5

43. Patel, K., Batish, A., Bhattacharya, A.: Optimization of surface roughness in an end-milling operation using nested experimental design. Prod. Eng. **3**(4–5), 361–373 (2009). https://doi.org/10.1007/s11740-009-0177-x

44. Sivasakthivel, P.S., Sudhakaran, R.: Optimization of machining parameters on temperature rise in end milling of Al 6063 using response surface methodology and genetic algorithm. Int. J. Adv. Manuf. Technol. **67**(9–12), 2313–2323 (2013). https://doi.org/10.1007/s00170-012-4652-8

45. Routara, B.C., Bandyopadhyay, A., Sahoo, P.: Roughness modeling and optimization in CNC end milling using response surface method: effect of workpiece material variation. Int. J. Adv. Manuf. Technol. **40**(11–12), 1166–1180 (2009). https://doi.org/10.1007/s00170-008-1440-6

46. Camposeco-Negrete, C.: Optimization of cutting parameters using response surface method for minimizing energy consumption and maximizing cutting quality in turning of AISI 6061 T6 aluminum. J. Clean. Prod. **91**, 109–117 (2015). https://doi.org/10.1016/j.jclepro.2014.12.017

47. Balogun, V.A., Mativenga, P.T.: Specific energy based characterization of surface integrity in mechanical machining. Proced. Manuf. **7**, 290–296 (2017). https://doi.org/10.1016/j.promfg.2016.12.072

48. Calvanese, M.L., Albertelli, P., Matta, A., Taisch, M., Milano, P.: Analysis of energy consumption in CNC machining centers and determination of optimal cutting conditions. (2013).

49. Camposeco-Negrete, C.: Optimization of cutting parameters for minimizing energy consumption in turning of AISI 6061 T6 using Taguchi methodology and ANOVA. J. Clean. Prod. **53**, 195–203 (2013). https://doi.org/10.1016/j.jclepro.2013.03.049+

50. Yusoff, A.R., Arsyad, F.: Evaluation of surface roughness and power consumption in machining FCD 450 cast iron using coated and uncoated irregular milling tools. IOP Conf. Ser. Mater. Sci. Eng. **114**, 012017 (2016). https://doi.org/10.1088/1757-899X/114/1/012017

51. Altıntaş, R.S., Kahya, M., Ünver, H.Ö.: Modelling and optimization of energy consumption for feature based milling. Int. J. Adv. Manuf. Technol. **86**(9–12), 3345–3363 (2016). https://doi.org/10.1007/s00170-016-8441-7

52. Kumar, R., Bilga, P.S., Singh, S.: Multi objective optimization using different methods of assigning weights to energy consumption responses, surface roughness and material removal rate during rough turning operation. J. Clean. Prod. **164**, 45–57 (2017). https://doi.org/10.1016/j.jclepro.2017.06.077

53. Iqbal, M., Konneh, M., Bin, M.H., Abdallah, K.A., Bin Binting, M.F.: Cutting temperature in high speed milling of silicon carbide using diamond coated tool. Int. J. Mech. Prod. Eng. **3**(4), 62–66 (2015)

54. Kus, A., Yahya Isik, M., Cakir, S.C., Özdemir, K.: Thermocouple and infrared sensor-based measurement of temperature distribution in metal cutting. Sensors **15**(1), 1274–1291 (2015). https://doi.org/10.3390/s150101274

55. Gosai, M., Bhavsar, S.N.: Experimental study on temperature measurement in turning operation of hardened steel (EN36). Proced. Technol. **23**, 311–318 (2016). https://doi.org/10.1016/j.protcy.2016.03.032

56. Patel, C.H., Patel, C.P.: Parametric optimization of end milling of AISI 1018 mild steel by various lubricants with solid carbide end mills. Int. J. Eng. Res. Appl. **3**, 728–732 (2013)

57. Patel, B., Nayak, H., Araniya, K., Champaneri, G.: Parametric optimization of temperature during CNC end milling of mild steel using RSM. Int. J. Eng. Res. Technol. **3**(1), 69–73 (2014)

58. Bhardwaj, B., Kumar, R., Singh, P.K.: An improved surface roughness prediction model using Box-Cox transformation with RSM in end milling of EN 353. J. Mech. Sci. Technol. **28**, 5149–5157 (2014). https://doi.org/10.1007/s12206-014-0837-4

59. Reddy, N.S.K., Rao, P.V.: A genetic algorithmic approach for optimization of surface roughness prediction model in dry milling. Mach. Sci. Technol. **9**(1), 63–84 (2005). https://doi.org/10.1081/MST-200051263

60. Singh, C., Bhogal, S.S., Pabla, D.B., Kumar, P.: Empirical modeling of surface roughness and metal removal rate in CNC milling operation. Int. J. Innov. Technol. Res. (JITR) **2**, 1120–1126 (2014)

61. Derringer, G., Suich, R.: Simultaneous optimization of several response variables. J. Qual. Technol. **12**(4), 214–219 (1980)

62. Jenarthanan, M.P., Jeyapaul, R.: Optimisation of machining parameters on milling of GFRP composites by desirability function analysis using Taguchi method. Int. J. Eng. Sci. Technol. **5**(4), 23–36 (2013)

63. Pattanaik, L.N.: Analytical Tools in Research, 1st edn. Educreation Publishing, Delhi (2017)

64. Kamguem, R., Djebara, A., Songmene, V.: Investigation on surface finish and metallic particle emission during machining of aluminum alloys using response surface methodology and desirability functions. Int. J. Adv. Manuf. Technol. **69**(5–8), 1283–1298 (2013). https://doi.org/10.1007/s00170-013-5105-8

65. Montgomery, D.C.: Design and Analysis of Experiments. Willey, New York (2009)

66. Kivak, T.: Optimization of surface roughness and flank wear using the Taguchi method in milling of Hadfield steel with PVD and CVD coated inserts. Measurement (London) **50**(1), 19–28 (2014). https://doi.org/10.1016/j.measurement.2013.12.017